A Robust Finite Difference Scheme for Strongly Coupled Systems of Singularly Perturbed Convection-diffusion Equations

Po-Wen Hsieh, Suh-Yuh Yang, and Cheng-Shu You
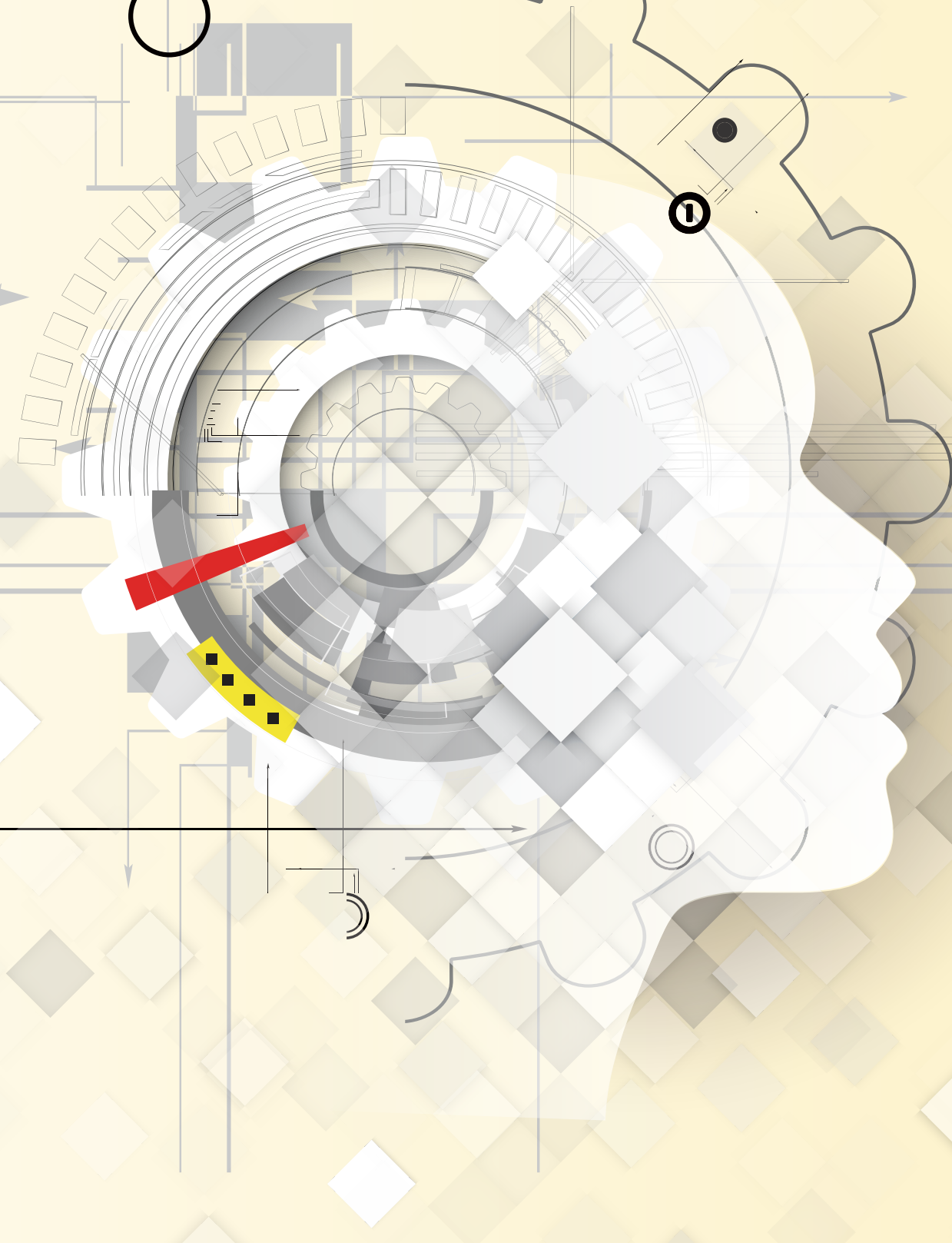
A robust finite difference scheme for strongly coupled systems of singularly perturbed convection-diffusion equations

Po-Wen Hsieh[1], Suh-Yuh Yang[2], and Cheng-Shu You[3]

Abstract

This paper is devoted to developing an Il'in-Allen-Southwell (IAS) parameter-uniform difference scheme on uniform meshes for solving strongly coupled systems of singularly perturbed convection-diffusion equations whose solutions may display boundary and/or interior layers, where strong coupling means that the solution components in the system are coupled together mainly through their first derivatives. By decomposing the coefficient matrix of convection term into the Jordan canonical form, we first construct an IAS scheme for 1-D systems and then extend the scheme to 2-D systems by employing an alternating direction technique. The robustness of the developed IAS scheme is illustrated through a series of numerical examples, including the magnetohydrodynamic duct flow problem with a high Hartmann number. Numerical evidence indicates that the IAS scheme appears to be formally second order accurate in the sense that it is second order convergent when the perturbation parameter ε is not too small and when ε is sufficiently small, the scheme is first order convergent in the discrete maximum norm uniformly in ε.

Keywords: strongly coupled system, singularly perturbed convection-diffusion equation, boundary and interior layers, magnetohydrodynamic duct flow, Il'in-Allen-Southwell scheme, uniform convergence

AMS subject classifications (2010): 65N06, 65N12, 76M20

Running title: A difference scheme for strongly coupled systems

1 Introduction

Nowadays, solving singularly perturbed convection-diffusion equations is still one of the most challenging tasks in the numerical approximation of differential equations, since most conventional numerical techniques often lead to discretizations that are unrealistic and worthless when the singular perturbation parameter is sufficiently small compared with the modulus of the convection [19, 26, 27]. Consequently, in the development of efficient numerical methods for solving singularly perturbed problems, we are interested in robust methods that work for all values of the perturbation parameter. Toward this aim, in this paper we are going to develop a robust

---

[1]Department of Applied Mathematics, National Chung Hsing University, South District, Taichung City 40227, Taiwan. E-mail address: pwhsieh@nchu.edu.tw

[2]Corresponding author. Department of Mathematics, National Central University, Jhongli District, Taoyuan City 32001, Taiwan; also affiliated with National Center for Theoretical Sciences, National Taiwan University, Da'an District, Taipei City 10617, Taiwan. E-mail address: syyang@math.ncu.edu.tw

[3]Department of Mathematics, National Central University, Jhongli District, Taoyuan City 32001, Taiwan. E-mail address: csdyou@gmail.com

finite difference scheme for solving the following system of singularly perturbed convection-diffusion equations:

$$\begin{cases} -\varepsilon \Delta u - A u_x - B u_y + C u &= f \quad \text{in } \Omega, \\ u &= g \quad \text{on } \partial\Omega, \end{cases} \tag{1.1}$$

where, for simplicity, $\Omega := (0,1) \times (0,1)$ is the considered domain and its boundary is denoted by $\partial\Omega$; $u = (u_1, u_2, \cdots, u_n)^\top$ is the physical quantity of interest; ε is the perturbation parameter with $0 < \varepsilon \ll 1$; $A = (a_{ij}(x,y))_{n \times n}$ and $B = (b_{ij}(x,y))_{n \times n}$ are the given coefficient matrices of the convection terms and $C = (c_{ij}(x,y))_{n \times n}$ is the reaction coefficient matrix; $f = (f_1, f_2, \cdots, f_n)^\top$ is the given source and $g = (g_1, g_2, \cdots, g_n)^\top$ is the prescribed boundary data. In this paper, we will focus on the strongly coupled system of convection-diffusion type, i.e., A or B is nontrivial such that the solution components in the system $u_1, u_2, \cdots, u_n$ are coupled together mainly through their first derivatives. The analytical behavior of the solution of a singularly perturbed boundary value problem depends on the nature of the boundary conditions and it was pointed out in [27] that the most difficult case is when these conditions are of Dirichlet type.

The coupled system (1.1) of singularly perturbed convection-diffusion equations can model more complicated physical phenomena when compared with the scalar case. Some typical examples include the turbulent interaction of waves and currents [32], the diffusion processes in the presence of chemical reactions [28], the optimal control and certain resistance-capacitor electrical circuits [11], and the magnetohydrodynamic duct flow problems [3, 5, 6], etc. It is well known that when the perturbation parameter ε is small enough than the modulus of the convection, each solution component may display different strong boundary and/or interior layers. These layers are narrow regions in the domain Ω where the solution component changes rapidly. However, it is often difficult to resolve numerically the high gradients near the layer regions. Consequently, this simple coupled system (1.1) has been the focus of intense research for quite some time, see e.g., [8, 9, 14, 15, 16, 17, 18, 20, 21, 22, 30] and references cited therein.

Most conventional numerical methods for solving singularly perturbed problems are lacking in either stability or accuracy (cf. [19, 27, 31]). For example, when the mesh size is not small compared to the perturbation parameter, the usual central difference scheme performs very poorly since large spurious oscillations appear not only near the layer regions but also in the others. The exotic behaviors of various numerical methods for scalar singularly perturbed convection-diffusion equations can be found in [1]. To overcome this difficulty in solving singularly perturbed system (1.1), only few stable and accurate numerical methods have been developed. For the 1-D convection-diffusion type, O'Riordan and Stynes [20] proposed a difference scheme which is consisting of simple upwinding and an appropriate piecewise-uniform Shishkin mesh. They showed the first-order convergence when $n = 2$, A is a strictly diagonally dominant M-matrix and $C = 0$. In [21], with proper hypotheses placed on the coupling matrices A and C, a similar scheme can be applied to the case of $n \geq 2$. Also, they obtained the first-order approximations by using a Jacobi-type iteration [22]. For the 2-D convection-diffusion type, when $n = 2$, A and B are symmetry matrices with zero diagonal entries and $C = 0$, we proposed in [5] a compact difference scheme with accuracy of $O(\varepsilon^2 h + \varepsilon h^2 + h^3)$, where h denotes the mesh parameter. We remark that all these methods only have order one accuracy, because the upwinding is the major ingredient of the methods. It is well known that the simple upwind scheme has a good stability for singularly perturbed convection-diffusion problems. However,

2

its convergence is not uniform in the perturbation parameter ε in the discrete maximum norm [27]. Although one can probably design some certain layer-adapted meshes [12, 13, 20, 28, 29] to achieve the uniform convergence property, it seems not an easy task because until now not much is known in the literature about the structure of layers of the strongly coupled system (1.1), see [24, 26] and many references cited therein.

One of the most successful numerical methods for scalar singularly perturbed convection-diffusion equations is the so-called Il'in-Allen-Southwell (IAS) parameter-uniform scheme [23, 27], which retains the upwinding effect in its mechanism. The IAS scheme is an exponentially fitted finite difference scheme with a formally second-order accuracy. More precisely, it is a second order accurate scheme when the perturbation parameter ε is not too small. As ε is getting small enough, the order of accuracy of the scheme will be decreased to first order; nevertheless, the convergence is uniform in ε in the discrete maximum norm under some appropriate conditions (cf. [2, 10, 25, 27]), i.e., no matter how small ε is, we always have $\|u - u_h\|_\infty \le Ch$ under some appropriate conditions, where C is a positive constant independent of ε and h. Although the IAS scheme is demonstrated to be efficient for obtaining stable and accurate numerical results for scalar singularly perturbed convection-diffusion equations, to the best of our knowledge, it has never been achieved before in the literature to successfully construct an effective IAS scheme for solving the strongly coupled system (1.1) of singularly perturbed convection-diffusion equations [16, 26]. Very recently, we proposed in [4] a novel technique to apply the IAS scheme for scalar equations to derive a formally second-order scheme for the strongly coupled system (1.1). However, the resulting scheme is suitable only for one-sided boundary layer problems. Numerical evidences show that the scheme developed in [4] converges uniformly in ε in the discrete maximum norm with appropriate piecewise-uniform Shishkin meshes [20], but it doesn't converge uniformly in ε with regular meshes.

In the present work, we will focus our attention on developing a new IAS scheme on uniform meshes for effectively solving the strongly coupled system (1.1). By decomposing the coefficient matrix of convection term into the Jordan canonical form, we first construct the IAS scheme for the 1-D case of coupled system (1.1). We then extend the scheme to the 2-D case by employing an alternating direction technique [4, 5]. The resulting IAS scheme is a formally second-order difference scheme over a five-point compact stencil and it is capable of solving two-sided boundary layer problems, see Example 4.1 below. We provide a series of numerical examples, including the coupled system of the magnetohydrodynamic duct flow equations, to illustrate the robustness of the developed IAS scheme. From the numerical results, we can find that as in the scalar case, the IAS scheme is second order accurate when the perturbation parameter ε is not too small; when the parameter ε is getting sufficiently small, the order of convergence deteriorates to first order, but the computed solutions converge uniformly in ε in the discrete maximum norm. In other words, the developed IAS scheme appears to be an ε-uniform difference scheme. This is the most attractive feature in developing difference schemes for numerically solving systems of singularly perturbed equations. Let us remark that we consider the uniform meshes in this paper only for simplicity. With a minor modification, a similar IAS scheme can be derived for non-uniform meshes (cf. [4]).

The rigorous convergence analysis of the developed IAS scheme in this paper is still an open problem. It seems a difficult task to prove the ε-uniform convergence of the IAS scheme, even for

the simpler case of 2-D scalar equation which has only recently been proved by Roos and Schopf [25]. As is well known, the discrete maximum principle is the main tool used in convergence proofs of finite difference schemes, but we do not expect that it will hold for the proposed IAS scheme. This is because it has already been pointed out in [20] that the continuous problem (1.1) does not in general satisfy the conventional maximum principle, see Example 2.1 in [20]. Indeed, numerical results reported in Section 4 below show that the newly proposed IAS scheme does not in general satisfy the conventional discrete maximum principle (cf. [33]).

The remainder of this paper is organized as follows. In section 2, we derive an IAS scheme for 1-D strongly coupled systems. With the help of an alternating direction technique, in section 3 we extend the scheme to 2-D systems using a five-point compact stencil. In section 4, a series of numerical examples are presented to illustrate the robustness of the developed IAS scheme. Finally, a brief summary and conclusions are drawn in section 5.

2 Il'in-Allen-Southwell scheme for 1-D system

In this section, we will derive an IAS scheme for the 1-D counterpart of the coupled system (1.1). We first consider the system without reaction term and the system with a reaction term will be addressed in Remark 2.3 at the end of this section. Let $0 = x_0 < x_1 < \cdots < x_m = 1$ be a uniform partition of $[0,1]$ with mesh size $h = 1/m$. For each subinterval $[x_{i-1}, x_{i+1}]$, we consider the following local approximate system and the unknown is still denoted by $\boldsymbol{u}(x)$:

$$-\varepsilon \boldsymbol{u}''(x) - \boldsymbol{A}(x_i)\boldsymbol{u}'(x) = \boldsymbol{f}(x), \quad x \in [x_{i-1}, x_{i+1}]. \tag{2.1}$$

For simplicity, we let $\boldsymbol{A} := \boldsymbol{A}(x_i)$. We also assume that the eigenvalues of $\boldsymbol{A}$ are all real, since we will mainly focus on (2.1) with a small perturbation parameter ε that is a nearly hyperbolic system. By the Jordan canonical form theorem [7], there exists an $n \times n$ real nonsingular matrix $\boldsymbol{P}$ constructed by the generalized eigenvectors of $\boldsymbol{A}$ such that

$$\boldsymbol{P}^{-1}\boldsymbol{A}\boldsymbol{P} = \boldsymbol{J} = \begin{bmatrix} J_1 & & & \\ & J_2 & & \\ & & \ddots & \\ & & & J_k \end{bmatrix}, \tag{2.2}$$

where all unspecified entries are zero and J_ℓ is a Jordan block corresponding to the eigenvalue λ_ℓ for $\ell = 1, 2, \cdots, k$. Moreover, each Jordan block J_ℓ can be expressed in the form

$$J_\ell = \lambda_\ell I_\ell + N_\ell, \tag{2.3}$$

where I_ℓ is an identity matrix and N_ℓ is a nilpotent matrix or a zero matrix, i.e.,

$$N_\ell = \begin{bmatrix} 0 & 1 & & \\ & 0 & \ddots & \\ & & \ddots & 1 \\ & & & 0 \end{bmatrix} \quad \text{or} \quad N_\ell = \boldsymbol{0}. \tag{2.4}$$

4

Now we define $v(x) := P^{-1}u(x)$ and $g(x) := P^{-1}f(x)$ for $x \in [x_{i-1}, x_{i+1}]$, then the 1-D local system (2.1) can be converted into the following form:

$$-\varepsilon v''(x) - J v'(x) = g(x), \quad x \in [x_{i-1}, x_{i+1}], \tag{2.5}$$

or equivalently,

$$
\begin{cases}
-\varepsilon v_1''(x) - J_1 v_1'(x) &= g_1(x), \quad x \in [x_{i-1}, x_{i+1}], \\
-\varepsilon v_2''(x) - J_2 v_2'(x) &= g_2(x), \quad x \in [x_{i-1}, x_{i+1}], \\
\quad\quad\quad\quad \vdots \\
-\varepsilon v_k''(x) - J_k v_k'(x) &= g_k(x), \quad x \in [x_{i-1}, x_{i+1}],
\end{cases}
\tag{2.6}
$$

with $v = [v_1, v_2, \cdots, v_k]^\top$ and $g = [g_1, g_2, \cdots, g_k]^\top$. Next, we are going to construct the IAS scheme for each subsystem in (2.6) at the grid point x_i. For $\ell = 1, 2, \cdots, k$, we have from (2.6) and (2.3) that

$$-\varepsilon v_\ell''(x) - \lambda_\ell v_\ell'(x) = g_\ell(x) + N_\ell v_\ell'(x), \quad x \in [x_{i-1}, x_{i+1}]. \tag{2.7}$$

We define the δ-operators, δ_x and δ_x^2, in the usual way

$$\delta_x w[i] := \frac{w[i+1] - w[i-1]}{2h} \quad \text{and} \quad \delta_x^2 w[i] := \frac{w[i+1] - 2w[i] + w[i-1]}{h^2}, \tag{2.8}$$

where $w[i]$ can be the function value $w(x_i)$ or its approximation w_i. By formally applying the IAS approach [27] to the subsystem (2.7) yields the pseudo-difference scheme

$$-\alpha_\ell \delta_x^2 v_\ell(x_i) - \lambda_\ell \delta_x v_\ell(x_i) = g_\ell(x_i) + N_\ell v_\ell'(x_i) + O(h^2), \tag{2.9}$$

where

$$
\alpha_\ell =
\begin{cases}
\dfrac{\lambda_\ell h}{2} \coth\left(\dfrac{\lambda_\ell h}{2\varepsilon}\right), & \text{if } \lambda_\ell \neq 0, \\
\varepsilon, & \text{if } \lambda_\ell = 0.
\end{cases}
\tag{2.10}
$$

Obviously, the term $N_\ell v_\ell'(x_i)$ on the right-hand side of (2.9) must be further approximated to reach a complete finite difference scheme. We also recognize that (2.9) is formally second-order accurate for approximating (2.7) at the grid point x_i, since the truncation error $O(h^2)$ may depend on the perturbation parameter ε.

Now, let us give a concrete example by considering the following simple case. Assume that

$$J = \lambda I + N := \begin{bmatrix} \lambda & 1 \\ 0 & \lambda \end{bmatrix}_{2 \times 2}, \quad \lambda \neq 0.$$

Then the strongly coupled system (2.5) becomes

$$-\varepsilon v''(x) - \lambda v'(x) = g(x) + N v'(x), \quad x \in [x_{i-1}, x_{i+1}], \tag{2.11}$$

where $v = (v_1, v_2)^\top$ and $g = (g_1, g_2)^\top$. Applying the IAS approach to (2.11) at the nodal point x_i yields

$$
\begin{cases}
-\alpha \delta_x^2 v_1(x_i) - \lambda \delta_x v_1(x_i) &= g_1(x_i) + v_2'(x_i) + O(h^2), \\
-\alpha \delta_x^2 v_2(x_i) - \lambda \delta_x v_2(x_i) &= g_2(x_i) + O(h^2),
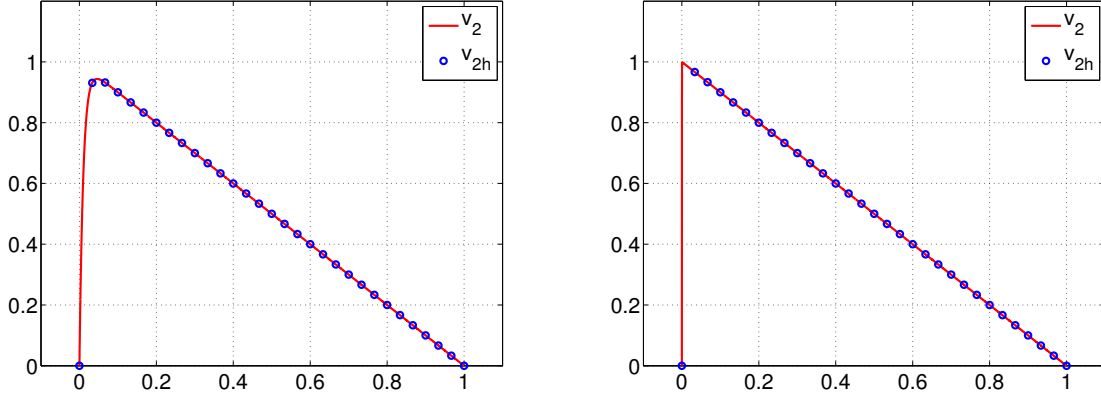\end{cases}
\tag{2.12}
$$

5

Figure 2.1: The exact solution v_2 and its IAS finite difference solution v_{2h} of the two-point boundary value problem $-\varepsilon v_2''(x) - v_2'(x) = 1$ with $v_2(0) = v_2(1) = 0$. (left) $\varepsilon = 10^{-2}$ and $h = 1/30$; (right) $\varepsilon = 10^{-4}$ and $h = 1/30$.

where we have to approximate $v_2'(x_i)$ appropriately to achieve the ε-uniform difference scheme. However, when the perturbation parameter ε is very small, from the second equation in system (2.11), we know that there is probably a strong boundary or interior layer and v_2 has a large gradient there. Thus, it seems very difficult to find an ε-uniform difference approximation to $v_2'(x_i)$ using the nodal values of v_2 directly, even if we have the exact values of v_2 at the grid points near x_i. For example, we can observe from Figure 2.1 that finding a difference approximation to $v_2'(x)$ at the grid point x_1 by using the neighboring nodal values will strongly depend on the shape of the exact solution v_2, and hence depends on the perturbation parameter ε. It is clear that no matter we use upwind difference or central difference at x_1, we can not find an accurate approximation to $v_2'(x_1)$ uniformly in ε. Notice that if $\lambda = 0$, then the second equation in system (2.11) will reduce to $-\varepsilon v_2''(x) = g_2(x)$ for $x \in [x_{i-1}, x_{i+1}]$, and we use the usual central difference to approximate $v_2'(x_i)$.

In what follows, we are going to introduce a novel idea for the approximation of $N_\ell v_\ell'(x_i)$ in (2.9) such that the convergence of the resulting IAS scheme is uniform in ε in the discrete maximum norm. Assume that $\lambda_\ell \neq 0$ and $N_\ell \neq \mathbf{0}$. We define $\boldsymbol{r}_\ell(x) := \boldsymbol{g}_\ell(x) + N_\ell v_\ell'(x)$ and then consider the following approximate system of (2.7), where for simplicity the unknown is still denoted by $\boldsymbol{v}_\ell(x)$:

$$-\varepsilon \boldsymbol{v}_\ell''(x) - \lambda_\ell \boldsymbol{v}_\ell'(x) = \boldsymbol{r}_\ell(x_i), \quad x \in [x_{i-1}, x_{i+1}]. \tag{2.13}$$

One can easily verify that the general solution of (2.13) is given by

$$\boldsymbol{v}_\ell(x) = -\frac{\boldsymbol{r}_\ell(x_i)}{\lambda_\ell}(x - x_i) + \boldsymbol{d}_1 e^{-\lambda_\ell(x-x_i)/\varepsilon} + \boldsymbol{d}_2, \tag{2.14}$$

for some constant vectors $\boldsymbol{d}_1$ and $\boldsymbol{d}_2$. Now, taking the two endpoints $x = x_{i+1}$ and $x = x_{i-1}$, we

6

have

$$
\begin{cases}
v_\ell(x_{i+1}) &= -\dfrac{r_\ell(x_i)}{\lambda_\ell}h + d_1 e^{-\lambda_\ell h/\varepsilon} + d_2, \\[3mm]
v_\ell(x_{i-1}) &= \dfrac{r_\ell(x_i)}{\lambda_\ell}h + d_1 e^{\lambda_\ell h/\varepsilon} + d_2.
\end{cases}
\tag{2.15}
$$

Solving (2.15) for d_1 and d_2, we obtain

$$
\begin{cases}
d_1 &= \dfrac{v_\ell(x_{i+1}) - v_\ell(x_{i-1}) + \frac{2h r_\ell(x_i)}{\lambda_\ell}}{e^{-\lambda_\ell h/\varepsilon} - e^{\lambda_\ell h/\varepsilon}}, \\[4mm]
d_2 &= \dfrac{\left(v_\ell(x_{i+1}) + \frac{r_\ell(x_i)}{\lambda_\ell}h\right)e^{\lambda_\ell h/\varepsilon} - \left(v_\ell(x_{i-1}) - \frac{r_\ell(x_i)}{\lambda_\ell}h\right)e^{-\lambda_\ell h/\varepsilon}}{e^{\lambda_\ell h/\varepsilon} - e^{-\lambda_\ell h/\varepsilon}},
\end{cases}
\tag{2.16}
$$

and this combining with (2.14) implies

$$
\begin{aligned}
v'_\ell(x_i) &= -\frac{r_\ell(x_i)}{\lambda_\ell} - \frac{d_1 \lambda_\ell}{\varepsilon} \\[2mm]
&= \left(-\frac{1}{\lambda_\ell} - \frac{2h}{\varepsilon(e^{-\lambda_\ell h/\varepsilon} - e^{\lambda_\ell h/\varepsilon})}\right)r_\ell(x_i) - \frac{2h\lambda_\ell}{\varepsilon(e^{-\lambda_\ell h/\varepsilon} - e^{\lambda_\ell h/\varepsilon})}\delta_x v_\ell(x_i).
\end{aligned}
\tag{2.17}
$$

Define

$$
s_\ell := -\frac{1}{\lambda_\ell} - \frac{h}{\varepsilon \sinh(-\lambda_\ell h/\varepsilon)} \quad \text{and} \quad t_\ell := -\frac{h\lambda_\ell}{\varepsilon \sinh(-\lambda_\ell h/\varepsilon)}.
\tag{2.18}
$$

Then we obtain from (2.17) and (2.18) that

$$
\begin{aligned}
v'_\ell(x_i) &= \left(-\frac{1}{\lambda_\ell} - \frac{h}{\varepsilon \sinh(-\lambda_\ell h/\varepsilon)}\right)r_\ell(x_i) + \frac{-h\lambda_\ell}{\varepsilon \sinh(-\lambda_\ell h/\varepsilon)}\delta_x v_\ell(x_i) \\[2mm]
&= s_\ell r_\ell(x_i) + t_\ell \delta_x v_\ell(x_i),
\end{aligned}
\tag{2.19}
$$

We now deal with the term $g_\ell(x_i) + N_\ell v'_\ell(x_i)$ on the right-hand side of (2.9). From (2.19) with $r_\ell(x_i) = g_\ell(x_i) + N_\ell v'_\ell(x_i)$, we have

$$
\begin{aligned}
&g_\ell(x_i) + N_\ell v'_\ell(x_i) \\
&= g_\ell(x_i) + N_\ell\Big(s_\ell r_\ell(x_i) + t_\ell \delta_x v_\ell(x_i)\Big) \\
&= g_\ell(x_i) + s_\ell N_\ell g_\ell(x_i) + t_\ell N_\ell \delta_x v_\ell(x_i) + s_\ell N_\ell^2 v'_\ell(x_i) \\
&= g_\ell(x_i) + s_\ell N_\ell g_\ell(x_i) + t_\ell N_\ell \delta_x v_\ell(x_i) + s_\ell N_\ell^2\Big(s_\ell r_\ell(x_i) + t_\ell \delta_x v_\ell(x_i)\Big) \\
&= g_\ell(x_i) + \big(s_\ell N_\ell + s_\ell^2 N_\ell^2\big)g_\ell(x_i) + \big(t_\ell N_\ell + s_\ell t_\ell N_\ell^2\big)\delta_x v_\ell(x_i) + s_\ell^2 N_\ell^3 v'_\ell(x_i).
\end{aligned}
\tag{2.20}
$$

Repeating the above process and using the fact that N_ℓ is a nilpotent matrix, we obtain

$$
\begin{aligned}
g_\ell(x_i) + N_\ell v'_\ell(x_i) &= g_\ell(x_i) + \Big(s_\ell N_\ell + s_\ell^2 N_\ell^2 + \cdots + s_\ell^{p_\ell-1} N_\ell^{p_\ell-1}\Big)g_\ell(x_i) \\
&\quad + \Big(t_\ell N_\ell + s_\ell t_\ell N_\ell^2 + \cdots + s_\ell^{p_\ell-2} t_\ell N_\ell^{p_\ell-1}\Big)\delta_x v_\ell(x_i) \\
&= g_\ell(x_i) + N_\ell\Big(s_\ell I_\ell + s_\ell^2 N_\ell + \cdots + s_\ell^{p_\ell-1} N_\ell^{p_\ell-2}\Big)g_\ell(x_i) \\
&\quad + N_\ell\Big(t_\ell I_\ell + s_\ell t_\ell N_\ell + \cdots + s_\ell^{p_\ell-2} t_\ell N_\ell^{p_\ell-2}\Big)\delta_x v_\ell(x_i) \\
&:= g_\ell(x_i) + N_\ell S_\ell g_\ell(x_i) + N_\ell T_\ell \delta_x v_\ell(x_i),
\end{aligned}
\tag{2.21}
$$

where $p_\ell \times p_\ell$ is the matrix size of N_ℓ and we define

$$
\begin{aligned}
S_\ell &:= s_\ell I_\ell + s_\ell^2 N_\ell + \cdots + s_\ell^{p_\ell-1} N_\ell^{p_\ell-2}, \\
T_\ell &:= t_\ell I_\ell + s_\ell t_\ell N_\ell + \cdots + s_\ell^{p_\ell-2} t_\ell N_\ell^{p_\ell-2}.
\end{aligned}
$$

Substituting (2.21) into the right-hand side of (2.9) yields

$$
-\alpha_\ell \delta_x^2 v_\ell(x_i) - (\lambda_\ell I_\ell + N_\ell T_\ell)\delta_x v_\ell(x_i) = g_\ell(x_i) + N_\ell S_\ell g_\ell(x_i) + O(h^2). \tag{2.22}
$$

Recall that $v = [v_1, v_2, \cdots, v_k]^\top$ and $g = [g_1, g_2, \cdots, g_k]^\top$. Let v_ℓ^i denote the approximation of $v_\ell(x_i)$ and define $v^i := [v_1^i, v_2^i, \cdots, v_k^i]^\top$. Dropping the local truncation error term in (2.22), we arrive at the following IAS scheme for the 1-D coupled system (2.5) at the grid point x_i:

$$
-\alpha \delta_x^2 v^i - (\Lambda + NT)\delta_x v^i = g(x_i) + NSg(x_i), \tag{2.23}
$$

where the involved matrices are given by

$$
\alpha = \begin{bmatrix} \alpha_1 I_1 & & & \\ & \alpha_2 I_2 & & \\ & & \ddots & \\ & & & \alpha_k I_k \end{bmatrix}, \quad
\Lambda = \begin{bmatrix} \lambda_1 I_1 & & & \\ & \lambda_2 I_2 & & \\ & & \ddots & \\ & & & \lambda_k I_k \end{bmatrix},
$$

$$
N = \begin{bmatrix} N_1 & & & \\ & N_2 & & \\ & & \ddots & \\ & & & N_k \end{bmatrix}, \quad
T = \begin{bmatrix} T_1 & & & \\ & T_2 & & \\ & & \ddots & \\ & & & T_k \end{bmatrix}, \quad
S = \begin{bmatrix} S_1 & & & \\ & S_2 & & \\ & & \ddots & \\ & & & S_k \end{bmatrix}. \tag{2.24}
$$

Since $v(x) := P^{-1}u(x)$ and $g(x) := P^{-1}f(x)$ for $x \in [x_{i-1}, x_{i+1}]$, we define $v^i := P^{-1}u^i$. Then from (2.23), we obtain the IAS scheme for the 1-D coupled system (2.1) at the grid point x_i,

$$
-P\alpha P^{-1}\delta_x^2 u^i - P(\Lambda + NT)P^{-1}\delta_x u^i = P(I + NS)P^{-1}f(x_i), \tag{2.25}
$$

or equivalently,

$$
-P(I + NS)^{-1}\alpha P^{-1}\delta_x^2 u^i - P(I + NS)^{-1}(\Lambda + NT)P^{-1}\delta_x u^i = f(x_i), \tag{2.26}
$$

which is a formally second-order finite difference scheme. We remark that all the matrices in (2.26) depend on the grid point x_i, since we define $A = A(x_i)$.

From the numerical results reported in Section 4 below, we can find that as in the scalar case, the IAS scheme (2.26) seems to be second order convergent when the perturbation parameter ε is not too small and when the ε is sufficiently small, the scheme appears to be first order convergent in the discrete maximum norm uniformly in ε.

Remark 2.1. *The recursive expression of $v_\ell'(x_i)$ in (2.19) is very different from the direct approximations of $v_\ell'(x_i)$ using the nodal values of v_ℓ, which usually produce very poor results when x_i is located in the layer region. Moreover, from (2.18), we can find that*

$$
\lim_{\varepsilon \to 0^+} s_\ell = \lim_{\varepsilon \to 0^+} \left(-\frac{1}{\lambda_\ell} - \frac{h}{\varepsilon \sinh(-\lambda_\ell h/\varepsilon)} \right) = -\frac{1}{\lambda_\ell}, \tag{2.27}
$$

$$
\lim_{\varepsilon \to 0^+} t_\ell = \lim_{\varepsilon \to 0^+} \frac{-h\lambda_\ell}{\varepsilon \sinh(-\lambda_\ell h/\varepsilon)} = 0. \tag{2.28}
$$

This shows that

$$\lim_{\varepsilon \to 0^+} v_\ell'(x_i) = -\frac{1}{\lambda_\ell} r_\ell(x_i), \tag{2.29}$$

which is consistent with equation (2.13) as $\varepsilon \to 0^+$.

Remark 2.2. *If A is diagonalizable, say*

$$P^{-1}AP = \Lambda = \begin{bmatrix} \lambda_1 I_1 & & & \\ & \lambda_2 I_2 & & \\ & & \ddots & \\ & & & \lambda_k I_k \end{bmatrix}, \tag{2.30}$$

that is, $N_\ell = \mathbf{0}$ in (2.3) for all $\ell = 1, 2, \cdots, k$, then the IAS scheme (2.26) will be reduced to

$$-P\alpha P^{-1}\delta_x^2 u^i - P\Lambda P^{-1}\delta_x u^i = f(x_i), \tag{2.31}$$

or equivalently,

$$-P\alpha P^{-1}\delta_x^2 u^i - A\delta_x u^i = f(x_i). \tag{2.32}$$

Moreover, we can verify that the difference scheme (2.32) will converge to the 1-D system (2.1) at the grid point x_i as $h \to 0^+$.

Remark 2.3. *We now consider the 1-D coupled system with a reaction term:*

$$-\varepsilon u''(x) - A(x_i)u'(x) + C(x)u(x) = f(x), \quad x \in [x_{i-1}, x_{i+1}]. \tag{2.33}$$

We first rewrite (2.33) as

$$-\varepsilon u''(x) - A(x_i)u'(x) = f(x) - C(x)u(x) := \widetilde{f}(x), \quad x \in [x_{i-1}, x_{i+1}]. \tag{2.34}$$

Let $C := C(x_i)$. Then from (2.26), we have the following IAS difference scheme for (2.34):

$$-P(I + NS)^{-1}\alpha P^{-1}\delta_x^2 u^i - P(I + NS)^{-1}(\Lambda + NT)P^{-1}\delta_x u^i = \widetilde{f}(x_i) = f(x_i) - Cu(x_i), \tag{2.35}$$

which leads to

$$-P(I + NS)^{-1}\alpha P^{-1}\delta_x^2 u^i - P(I + NS)^{-1}(\Lambda + NT)P^{-1}\delta_x u^i + Cu^i = f(x_i). \tag{2.36}$$

3 Alternating direction technique for 2-D system

In this section, we will apply an alternating direction technique [4, 5] to extend the IAS finite difference scheme (2.26) to the 2-D strongly coupled system (1.1). Let $x_i = ih$ and $y_j = jh$ for $0 \le i, j \le m$, where $h = 1/m$ is the grid size in both the x- and y-directions, and let $\Omega_{ij} = [x_{i-1}, x_{i+1}] \times [y_{j-1}, y_{j+1}]$, $1 \le i, j \le m - 1$, be the (i, j)-cell centered at the point (x_i, y_j). We first

split the equation (1.1) into two separated 1-D convection-diffusion systems and approximate the coefficient matrices at the center point (x_i, y_j),

$$-\varepsilon u_{xx}(x,y) - A(x_i, y_j) u_x(x,y) = f_1(x,y) \quad \text{for } (x,y) \in \Omega_{ij}, \tag{3.1}$$

$$-\varepsilon u_{yy}(x,y) - B(x_i, y_j) u_y(x,y) = f_2(x,y) \quad \text{for } (x,y) \in \Omega_{ij}, \tag{3.2}$$

where the unknown function is still denoted by u and the functions f_1 and f_2 are defined by

$$f_1(x,y) := f(x,y) - \left(-\varepsilon u_{yy}(x,y) - B(x,y) u_y(x,y) + C(x,y) u(x,y) \right), \tag{3.3}$$

$$f_2(x,y) := f(x,y) - \left(-\varepsilon u_{xx}(x,y) - A(x,y) u_x(x,y) + C(x,y) u(x,y) \right). \tag{3.4}$$

Notice that the sum of (3.1) and (3.2) gives the original equation (1.1), except the convection coefficients are evaluated at the grid point (x_i, y_j), since

$$f_1 + f_2 = 2f - (-\varepsilon \Delta u - A u_x - B u_y + C u) - C u = f - C u. \tag{3.5}$$

Now, applying the IAS scheme (2.26) for 1-D systems to discretize (3.1) and (3.2) at (x_i, y_j) yields

$$-P_A (I + N_A S_A)^{-1} \alpha_A P_A^{-1} \delta_x^2 u^{ij} - P_A (I + N_A S_A)^{-1} (\Lambda_A + N_A T_A) P_A^{-1} \delta_x u^{ij} = f_1(x_i, y_j), \tag{3.6}$$

$$-P_B (I + N_B S_B)^{-1} \alpha_B P_B^{-1} \delta_y^2 u^{ij} - P_B (I + N_B S_B)^{-1} (\Lambda_B + N_B T_B) P_B^{-1} \delta_y u^{ij} = f_2(x_i, y_j). \tag{3.7}$$

Summing (3.6) and (3.7), we obtain the following difference scheme:

$$
\begin{aligned}
&-P_A (I + N_A S_A)^{-1} \alpha_A P_A^{-1} \delta_x^2 u^{ij} - P_A (I + N_A S_A)^{-1} (\Lambda_A + N_A T_A) P_A^{-1} \delta_x u^{ij} \\
&-P_B (I + N_B S_B)^{-1} \alpha_B P_B^{-1} \delta_y^2 u^{ij} - P_B (I + N_B S_B)^{-1} (\Lambda_B + N_B T_B) P_B^{-1} \delta_y u^{ij} \\
&+C u^{ij} = f(x_i, y_j),
\end{aligned}
\tag{3.8}
$$

which is the IAS scheme for the 2-D strongly coupled system (1.1) at the grid point (x_i, y_j). Again, all the matrices in (3.8) depend on the specific grid point (x_i, y_j).

4 Numerical experiments

In this section, we will present a series of numerical examples to illustrate the robustness of the developed IAS schemes (2.26) and (3.8) for solving 1-D and 2-D strongly coupled systems, respectively. We consider several examples exhibiting boundary layers, including the coupled system of the magnetohydrodynamic (MHD) duct flow equations [5, 6]. In particular, a 1-D nonlinearly and strongly coupled system of viscous Burgers' equations displaying interior layer behavior is also demonstrated in Example 4.4 below.

Example 4.1 *(1-D problem with a diagonalizable convection coefficient matrix)*. We consider a 1-D strongly coupled system,

$$
-\varepsilon \begin{bmatrix} u_1'' \\ u_2'' \\ u_3'' \end{bmatrix} - A \begin{bmatrix} u_1' \\ u_2' \\ u_3' \end{bmatrix} = \begin{bmatrix} -1 + \varepsilon x + 3x^3 \\ \varepsilon x + 2x^3 \\ 1 + \varepsilon x + 3x^3 \end{bmatrix} \quad \text{in } I := (0,1) \tag{4.1}
$$

with the boundary conditions, $\boldsymbol{u}(0) = \boldsymbol{u}(1) = (0,0,0)^\top$, and the coefficient matrix A is given by

$$A = \begin{bmatrix} 1 & -3 & 2 \\ 1 & -2 & 1 \\ 2 & -3 & 1 \end{bmatrix}. \tag{4.2}$$

The eigenvalues of A are -1, 0, and 1. Thus, matrix A is diagonalizable. The analytic solution $\boldsymbol{u} = (u_1, u_2, u_3)^\top$ of this two-point boundary value problem is given by

$$\begin{cases} u_1(x) &= -\dfrac{3}{4}w_1(x) - \dfrac{3}{4}w_2(\varepsilon)\dfrac{e^{-x/\varepsilon}-1}{e^{-1/\varepsilon}-1} - x - \dfrac{e^{x/\varepsilon}-1}{e^{-1/\varepsilon}-1}e^{-1/\varepsilon} + \dfrac{x-x^3}{6}, \\ u_2(x) &= -\dfrac{1}{2}w_1(x) - \dfrac{1}{2}w_2(\varepsilon)\dfrac{e^{-x/\varepsilon}-1}{e^{-1/\varepsilon}-1} + \dfrac{x-x^3}{6}, \\ u_3(x) &= -\dfrac{3}{4}w_1(x) - \dfrac{3}{4}w_2(\varepsilon)\dfrac{e^{-x/\varepsilon}-1}{e^{-1/\varepsilon}-1} + x + \dfrac{e^{x/\varepsilon}-1}{e^{-1/\varepsilon}-1}e^{-1/\varepsilon} + \dfrac{x-x^3}{6}, \end{cases} \tag{4.3}$$

where w_1 and w_2 are defined as follows:

$$w_1(x) := x^4 - 4x^3\varepsilon + 12x^2\varepsilon^2 - 24x\varepsilon^3 \quad \text{and} \quad w_2(\varepsilon) := 24\varepsilon^3 - 12\varepsilon^2 + 4\varepsilon - 1. \tag{4.4}$$

One can verify that when the perturbation parameter ε is small enough, the solution components u_1 and u_3 display strong boundary layers at the both endpoints $x = 0$ and $x = 1$, while the solution component u_2 exhibits boundary layer only at the left endpoint $x = 0$, see Figure 4.1. Thus, this is a two-sided boundary layer problem and cannot be solved correctly by our previous scheme developed in [4].

The numerical results produced by the developed IAS scheme (2.26) for $\varepsilon = 2^{-2j}$ with $j = 0, 1, \cdots, 12$ and $h = 2^{-i}$ with $i = 5, 6, \cdots, 10$ are reported in Table 4.1, from which we can find that if ε is not too small, then the IAS solutions display a second-order convergence in the discrete maximum norm. As ε is getting small, the order of accuracy of the scheme will be decreased to first order and the first-order convergence appears to be uniform in ε. This is consistent with our expectation. We also depict the IAS solutions with $h = 1/64$ in Figure 4.1 for $\varepsilon = 10^{-2}$ and $\varepsilon = 10^{-6}$. We find that the numerical solutions produced by the developed IAS scheme can capture the strong boundary layers very well, even if ε is very small.

Let $\mathcal{M}\boldsymbol{U} = \boldsymbol{F}$ be the resulting linear system associated with the IAS scheme. Then we numerically find that $\|\mathcal{M}^{-1}\|_\infty \approx 18.1309 \not\leq 1$ when $\varepsilon = 2^{-10}$ and $h = 1/32$. This means that the IAS scheme does not satisfy the conventional discrete maximum principle [33] for this example.

Example 4.2 (*1-D problem with multiple eigenvalue* 1). We consider another 1-D strongly coupled system in which the convection coefficient matrix A cannot be diagonalized, but represented in a Jordan canonical form with eigenvalue 1 of multiplicity 2:

$$-\varepsilon \begin{bmatrix} u_1'' \\ u_2'' \end{bmatrix} - \begin{bmatrix} 3 & -1 \\ 4 & -1 \end{bmatrix} \begin{bmatrix} u_1' \\ u_2' \end{bmatrix} = \begin{bmatrix} 2x+2 \\ 4 \end{bmatrix} \quad \text{in } I := (0,1), \tag{4.5}$$

Table 4.1. Maximum errors of the IAS solutions of Example 4.1.

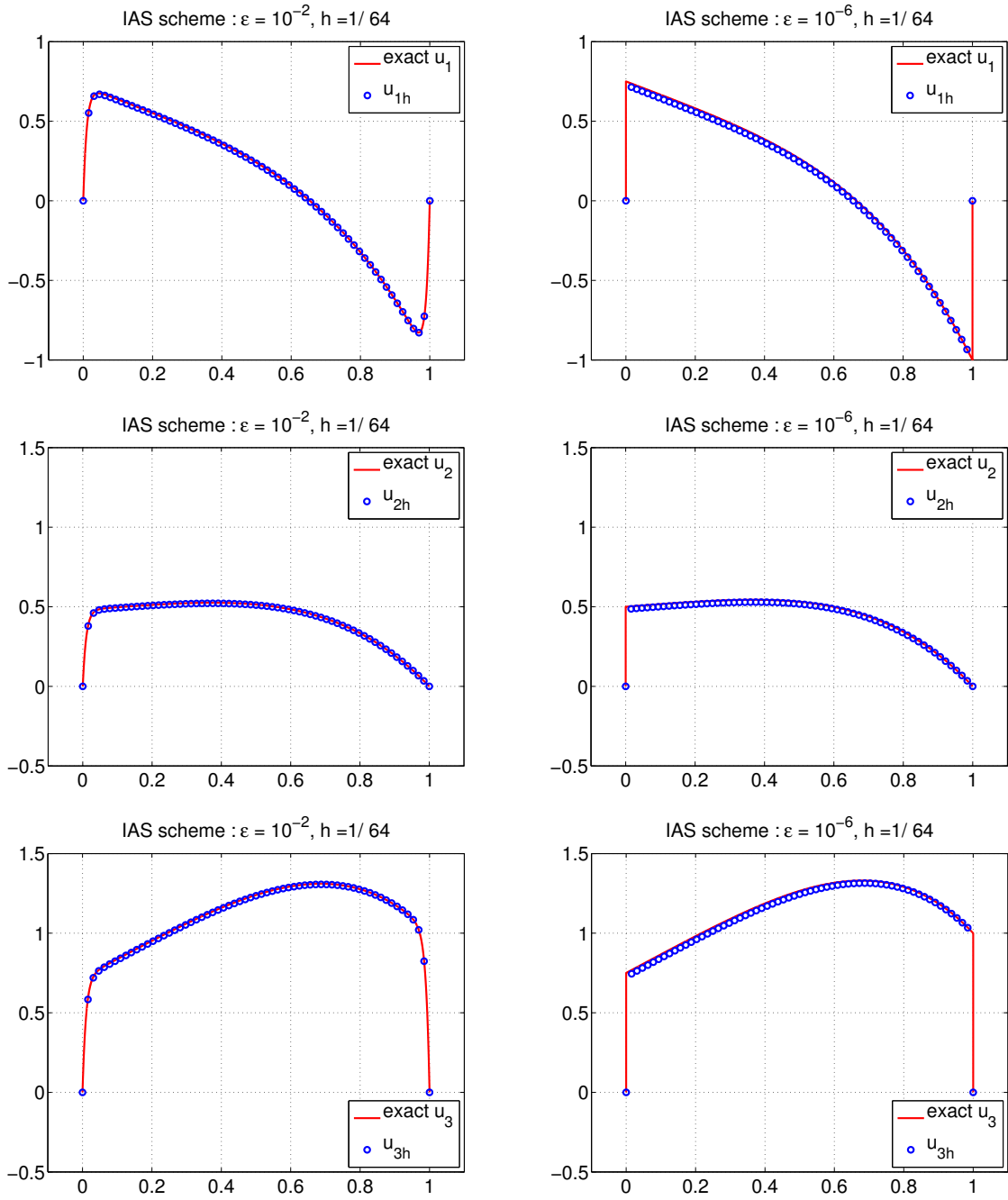|	ε	$h = 2^{-5}$	$h = 2^{-6}$	$h = 2^{-7}$	$h = 2^{-8}$	$h = 2^{-9}$	$h = 2^{-10}$	order
u_{1h}	1	1.2269e-04	3.0690e-05	7.6729e-06	1.9183e-06	4.7959e-07	1.1990e-07	2.00
	2^{-2}	7.4097e-04	1.8537e-04	4.6357e-05	1.1590e-05	2.8975e-06	7.2437e-07	2.00
	2^{-4}	3.7513e-03	9.4277e-04	2.3599e-04	5.9016e-05	1.4755e-05	3.6889e-06	2.00
	2^{-6}	1.4513e-02	3.8252e-03	9.6984e-04	2.4332e-04	6.0885e-05	1.5225e-05	1.98
	2^{-8}	3.4582e-02	1.2504e-02	3.6601e-03	9.6002e-04	2.4307e-04	6.0964e-05	1.83
	2^{-10}	4.3221e-02	2.0333e-02	8.7595e-03	3.1428e-03	9.1660e-04	2.4013e-04	1.50
	2^{-12}	4.5410e-02	2.2522e-02	1.0941e-02	5.1160e-03	2.1969e-03	7.8674e-04	1.17
	2^{-14}	4.5959e-02	2.3071e-02	1.1490e-02	5.6649e-03	2.7438e-03	1.2811e-03	1.03
	2^{-16}	4.6096e-02	2.3209e-02	1.1627e-02	5.8022e-03	2.8811e-03	1.4184e-03	1.00
	2^{-18}	4.6130e-02	2.3243e-02	1.1662e-02	5.8365e-03	2.9154e-03	1.4527e-03	1.00
	2^{-20}	4.6139e-02	2.3251e-02	1.1670e-02	5.8451e-03	2.9240e-03	1.4613e-03	1.00
	2^{-22}	4.6141e-02	2.3254e-02	1.1672e-02	5.8472e-03	2.9261e-03	1.4634e-03	1.00
	2^{-24}	4.6142e-02	2.3254e-02	1.1673e-02	5.8478e-03	2.9266e-03	1.4639e-03	1.00
u_{2h}	1	8.1790e-05	2.0460e-05	5.1153e-06	1.2789e-06	3.1972e-07	7.9931e-08	2.00
	2^{-2}	4.9398e-04	1.2358e-04	3.0904e-05	7.7264e-06	1.9316e-06	4.8292e-07	2.00
	2^{-4}	2.5008e-03	6.2852e-04	1.5732e-04	3.9344e-05	9.8368e-06	2.4592e-06	2.00
	2^{-6}	9.6753e-03	2.5501e-03	6.4656e-04	1.6222e-04	4.0590e-05	1.0150e-05	1.98
	2^{-8}	2.3055e-02	8.3361e-03	2.4401e-03	6.4001e-04	1.6205e-04	4.0642e-05	1.83
	2^{-10}	2.8814e-02	1.3555e-02	5.8397e-03	2.0952e-03	6.1107e-04	1.6009e-04	1.50
	2^{-12}	3.0273e-02	1.5015e-02	7.2941e-03	3.4107e-03	1.4646e-03	5.2449e-04	1.17
	2^{-14}	3.0639e-02	1.5381e-02	7.6599e-03	3.7766e-03	1.8292e-03	8.5404e-04	1.03
	2^{-16}	3.0731e-02	1.5472e-02	7.7515e-03	3.8681e-03	1.9207e-03	9.4557e-04	1.00
	2^{-18}	3.0754e-02	1.5495e-02	7.7744e-03	3.8910e-03	1.9436e-03	9.6846e-04	1.00
	2^{-20}	3.0759e-02	1.5501e-02	7.7801e-03	3.8967e-03	1.9493e-03	9.7418e-04	1.00
	2^{-22}	3.0761e-02	1.5502e-02	7.7815e-03	3.8981e-03	1.9507e-03	9.7561e-04	1.00
	2^{-24}	3.0761e-02	1.5503e-02	7.7819e-03	3.8985e-03	1.9511e-03	9.7597e-04	1.00
u_{3h}	1	1.2269e-04	3.0690e-05	7.6729e-06	1.9183e-06	4.7959e-07	1.1990e-07	2.00
	2^{-2}	7.4097e-04	1.8537e-04	4.6357e-05	1.1590e-05	2.8975e-06	7.2436e-07	2.00
	2^{-4}	3.7513e-03	9.4277e-04	2.3599e-04	5.9016e-05	1.4755e-05	3.6889e-06	2.00
	2^{-6}	1.4513e-02	3.8252e-03	9.6984e-04	2.4332e-04	6.0885e-05	1.5225e-05	1.98
	2^{-8}	3.4582e-02	1.2504e-02	3.6601e-03	9.6002e-04	2.4307e-04	6.0964e-05	1.83
	2^{-10}	4.3221e-02	2.0333e-02	8.7595e-03	3.1428e-03	9.1660e-04	2.4013e-04	1.50
	2^{-12}	4.5410e-02	2.2522e-02	1.0941e-02	5.1160e-03	2.1969e-03	7.8674e-04	1.17
	2^{-14}	4.5959e-02	2.3071e-02	1.1490e-02	5.6649e-03	2.7438e-03	1.2811e-03	1.03
	2^{-16}	4.6096e-02	2.3209e-02	1.1627e-02	5.8022e-03	2.8811e-03	1.4184e-03	1.00
	2^{-18}	4.6130e-02	2.3243e-02	1.1662e-02	5.8365e-03	2.9154e-03	1.4527e-03	1.00
	2^{-20}	4.6139e-02	2.3251e-02	1.1670e-02	5.8451e-03	2.9240e-03	1.4613e-03	1.00
	2^{-22}	4.6141e-02	2.3254e-02	1.1672e-02	5.8472e-03	2.9261e-03	1.4634e-03	1.00
	2^{-24}	4.6142e-02	2.3254e-02	1.1673e-02	5.8478e-03	2.9266e-03	1.4639e-03	1.00

Figure 4.1. The exact and IAS solutions of Example 4.1 with $\varepsilon = 10^{-2}$ and $\varepsilon = 10^{-6}$.

subject to the two-endpoint boundary conditions such that the analytic solution $\boldsymbol{u}$ is given by

$$
\begin{cases}
u_1(x) &= \dfrac{2e^{-1/\varepsilon}\{(-2x^2 + 2x + 2)\varepsilon + (8x - 4)\varepsilon^2 - 1\}}{(1 - e^{-1/\varepsilon})^2\varepsilon} + \dfrac{2e^{-x/\varepsilon}(-2x\varepsilon + x - 4\varepsilon^2)}{(1 - e^{-1/\varepsilon})^2\varepsilon} \\[2mm]
&\quad + \dfrac{2e^{-(x+1)/\varepsilon}\{x(2\varepsilon - 1) + 4\varepsilon^2 - 2\varepsilon + 1\}}{(1 - e^{-1/\varepsilon})^2\varepsilon} \\[2mm]
&\quad + \dfrac{2\{e^{-2/\varepsilon}x\varepsilon(x - 4\varepsilon - 1) - (x - 1)\varepsilon(4\varepsilon - x)\}}{(1 - e^{-1/\varepsilon})^2\varepsilon} \\[2mm]
&\quad + \dfrac{x(x - 2\varepsilon)e^{-1/\varepsilon} + (x - 1)(-x + 2\varepsilon - 1) + (2\varepsilon - 1)e^{-x/\varepsilon}}{1 - e^{-1/\varepsilon}}, \\[2mm]
u_2(x) &= \dfrac{4e^{-1/\varepsilon}\{(-2x^2 + 2x + 2)\varepsilon + (8x - 4)\varepsilon^2 - 1\}}{(1 - e^{-1/\varepsilon})^2\varepsilon} + \dfrac{4e^{-x/\varepsilon}(-2x\varepsilon + x - 4\varepsilon^2)}{(1 - e^{-1/\varepsilon})^2\varepsilon} \\[2mm]
&\quad + \dfrac{4e^{-(x+1)/\varepsilon}\{x(2\varepsilon - 1) + 4\varepsilon^2 - 2\varepsilon + 1\}}{(1 - e^{-1/\varepsilon})^2\varepsilon} \\[2mm]
&\quad + \dfrac{4\{e^{-2/\varepsilon}x\varepsilon(x - 4\varepsilon - 1) - (x - 1)\varepsilon(4\varepsilon - x)\}}{(1 - e^{-1/\varepsilon})^2\varepsilon}.
\end{cases} \tag{4.6}
$$

When the perturbation parameter ε is small enough, both the solution components u_1 and u_2 display strong boundary layers at the left endpoint $x = 0$.

The numerical results for $\varepsilon = 2^{-2j}$ with $j = 0, 1, \cdots, 12$ and $h = 2^{-i}$ with $i = 5, 6, \cdots, 10$ are reported in Table 4.2, which confirm our prediction. The elevation plots of the IAS solution in the boundary layer region with $h = 1/256$ for $\varepsilon = 10^{-3}$ are given in Figure 4.2. We find that the developed IAS scheme exhibits a high performance and the first-order convergence appears to be uniform in the perturbation parameter. Moreover, we numerically find that in general the criterion $\|\mathcal{M}^{-1}\|_\infty \leq 1$ does not hold, where $\mathcal{M}$ is the resulting matrix associated with the IAS scheme. For example, we have $\|\mathcal{M}^{-1}\|_\infty \approx 0.9688$ for $\varepsilon = 2^{-10}$ with $h = 1/32$, but $\|\mathcal{M}^{-1}\|_\infty \approx 4.9082$ for $\varepsilon = 2^{-5}$ with $h = 1/32$. Thus, the IAS scheme does not satisfy the discrete maximum principle [33] for this example.

Example 4.3 (*1-D problem with variable convection coefficients*). This example is taken from [20]. We consider the following 1-D strongly coupled system with variable convection coefficients:

$$
-\varepsilon \begin{bmatrix} u_1'' \\ u_2'' \end{bmatrix} - \begin{bmatrix} 4 + xe^x & -1 - 2x \\ -1 - x & 2 + x^2 \end{bmatrix} \begin{bmatrix} u_1' \\ u_2' \end{bmatrix} = \begin{bmatrix} -3x^2 - x - 1 \\ -2x + 1 \end{bmatrix} \quad \text{in } I := (0, 1) \tag{4.7}
$$

with the boundary conditions, $\boldsymbol{u}(0) = (2, 1)^\top$ and $\boldsymbol{u}(1) = (2, 2)^\top$. Since the exact solution is not available in this example, we use a reference solution $\boldsymbol{u}^* = (u_1^*, u_2^*)$ as the exact solution which is produced by the proposed IAS scheme over a uniform mesh with a small mesh size $h = 2^{-18} \approx 3.8147 \times 10^{-6}$. We find that when the perturbation parameter ε is small enough, both the reference solution components u_1^* and u_2^* display strong boundary layers at the left endpoint $x = 0$.

In this example, the eigenvalues $\lambda_{i\ell}$, $\ell = 1, 2$, of the variable coefficient matrix of convection term at each grid point x_i are approximately determined by using the MATLAB function `jordan(A)`, which finds the Jordan canonical form of the matrix. The numerical results for different perturbation parameters are collected in Table 4.3. We can find that the IAS scheme exhibits

Table 4.2. Maximum errors of the IAS solutions of Example 4.2.

|	ε	$h = 2^{-5}$	$h = 2^{-6}$	$h = 2^{-7}$	$h = 2^{-8}$	$h = 2^{-9}$	$h = 2^{-10}$	order
	1	5.9294e-05	1.4824e-05	3.7065e-06	9.2664e-07	2.3166e-07	5.7920e-08	2.00
	2^{-2}	6.8191e-04	1.7080e-04	4.2706e-05	1.0677e-05	2.6692e-06	6.6731e-07	2.00
	2^{-4}	3.4783e-03	8.7778e-04	2.2062e-04	5.5187e-05	1.3799e-05	3.4498e-06	2.00
	2^{-6}	1.1516e-02	3.3838e-03	9.1440e-04	2.3083e-04	5.7848e-05	1.4471e-05	1.93
	2^{-8}	7.7852e-03	3.6241e-03	2.9227e-03	8.5998e-04	2.3140e-04	5.8419e-05	1.41
	2^{-10}	2.4597e-02	9.6131e-03	2.0104e-03	9.1330e-04	7.3342e-04	2.1587e-04	1.37
u_{1h}	2^{-12}	2.8854e-02	1.3939e-02	6.2981e-03	2.4319e-03	5.0857e-04	2.2878e-04	1.40
	2^{-14}	2.9919e-02	1.5020e-02	7.3881e-03	3.5262e-03	1.5838e-03	6.0976e-04	1.12
	2^{-16}	3.0185e-02	1.5291e-02	7.6606e-03	3.7998e-03	1.8579e-03	8.8415e-04	1.02
	2^{-18}	3.0251e-02	1.5358e-02	7.7288e-03	3.8682e-03	1.9265e-03	9.5274e-04	1.00
	2^{-20}	3.0268e-02	1.5375e-02	7.7458e-03	3.8853e-03	1.9436e-03	9.6989e-04	0.99
	2^{-22}	3.0272e-02	1.5379e-02	7.7500e-03	3.8896e-03	1.9479e-03	9.7418e-04	0.99
	2^{-24}	3.0273e-02	1.5381e-02	7.7511e-03	3.8906e-03	1.9490e-03	9.7525e-04	0.99
	1	7.8605e-05	1.9663e-05	4.9157e-06	1.2290e-06	3.0725e-07	7.6813e-08	2.00
	2^{-2}	8.5143e-04	2.1332e-04	5.3338e-05	1.3336e-05	3.3341e-06	8.3352e-07	2.00
	2^{-4}	3.7673e-03	9.5394e-04	2.3925e-04	5.9860e-05	1.4968e-05	3.7422e-06	2.00
	2^{-6}	6.7265e-03	3.5655e-03	9.4083e-04	2.3842e-04	5.9808e-05	1.4965e-05	1.76
	2^{-8}	6.1006e-02	1.1371e-02	1.6545e-03	8.9039e-04	2.3514e-04	5.9602e-05	2.00
	2^{-10}	1.0596e-01	4.6143e-02	1.5622e-02	2.9234e-03	4.1192e-04	2.2254e-04	1.78
u_{2h}	2^{-12}	1.1731e-01	5.7678e-02	2.7130e-02	1.1673e-02	3.9380e-03	7.3735e-04	1.46
	2^{-14}	1.2015e-01	6.0562e-02	3.0037e-02	1.4591e-02	6.8226e-03	2.9268e-03	1.07
	2^{-16}	1.2086e-01	6.1283e-02	3.0764e-02	1.5321e-02	7.5536e-03	3.6585e-03	1.01
	2^{-18}	1.2103e-01	6.1463e-02	3.0945e-02	1.5503e-02	7.7363e-03	3.8415e-03	1.00
	2^{-20}	1.2108e-01	6.1508e-02	3.0991e-02	1.5549e-02	7.7820e-03	3.8872e-03	0.99
	2^{-22}	1.2109e-01	6.1520e-02	3.1002e-02	1.5560e-02	7.7934e-03	3.8986e-03	0.99
	2^{-24}	1.2109e-01	6.1522e-02	3.1005e-02	1.5563e-02	7.7963e-03	3.9015e-03	0.99
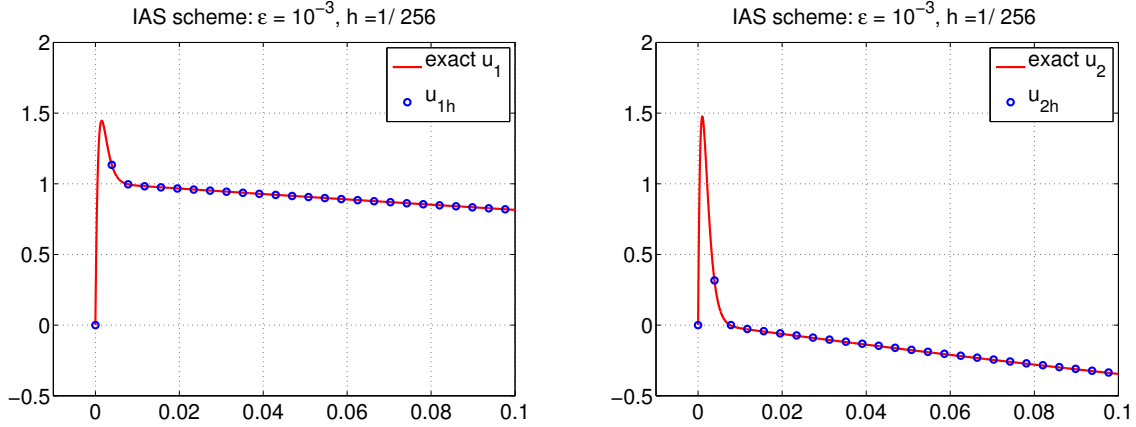
Figure 4.2. The magnifications of exact and IAS solutions for $h = 1/256$ near the boundary layer region of Example 4.2 with $\varepsilon = 10^{-3}$.

numerically the uniform convergence property in ε. The computed solutions using the IAS scheme with $h = 1/64$ for $\varepsilon = 10^{-4}$ are depicted in Figure 4.3. Again, the IAS scheme captures the strong boundary layers very well.

Example 4.4 (*1-D nonlinear problem of viscous Burgers' equations*). This example is quoted from [4]. We consider a two-point boundary value problem for the 1-D nonlinearly coupled system of viscous Burgers' equations,

$$-\varepsilon \left[\begin{array}{c} u_1'' \\ u_2'' \end{array} \right] - \left[\begin{array}{cc} -u_1 - u_2 & -u_1 \\ -u_2 & -u_1 - u_2 \end{array} \right] \left[\begin{array}{c} u_1' \\ u_2' \end{array} \right] = \left[\begin{array}{c} f_1 \\ f_2 \end{array} \right] \quad \text{in } I := (-1, 1). \tag{4.8}$$

We choose the source functions f_1 and f_2 such that the exact solution $\boldsymbol{u} = (u_1, u_2)^\top$ is given by

$$u_1(x) = -2 \tanh\left(\frac{x}{2\varepsilon}\right) \quad \text{and} \quad u_2(x) = -\tanh\left(\frac{x}{2\varepsilon}\right).$$

A direct iterative procedure is employed to linearize the nonlinear problem, in which the nonlinear terms $u_i u_j'$ are replaced by the approximations $u_{ih}^{(k)} u_j'$ in the $(k+1)$-th iteration with the initial functions $u_{1h}^{(0)}(x) := 5 \sin((x+1)\pi) - 2x$ and $u_{2h}^{(0)}(x) := 5 \sin((x+1)\pi) - x$. We then apply the IAS scheme (2.26) to solve the linearized problem at each iteration. The stopping criterion of the iterative procedure is the maximum difference between successive approximations smaller than or equal to 10^{-5}. We consider the nonlinearly coupled system with $\varepsilon = 10^{-\ell}$, $1 \le \ell \le 4$, on a uniform mesh with $h = 1/32$. The numerical results are depicted in Figure 4.4, where the iteration numbers are $16, 12, 2, 2$, respectively. From Figure 4.4, we can find that the proposed IAS scheme (2.26) can capture the interior layer structure very well.

Example 4.5 (*2-D MHD duct flow problem with analytic solution*). We consider a 2-D strongly coupled system of singularly perturbed convection-diffusion equations in $\Omega := (0, 1) \times (0, 1)$, which arises from the steady incompressible MHD duct flow problem with the Hartmann number $1/\varepsilon$

Table 4.3. Maximum errors of the IAS solutions of Example 4.3.

|	ε	$h = 2^{-5}$	$h = 2^{-6}$	$h = 2^{-7}$	$h = 2^{-8}$	$h = 2^{-9}$	$h = 2^{-10}$	order
	1	6.8714e-05	1.7184e-05	4.2982e-06	1.0765e-06	2.7102e-07	6.9660e-08	1.99
	2^{-2}	6.2008e-04	1.5579e-04	3.8999e-05	9.7544e-06	2.4404e-06	6.1169e-07	2.00
	2^{-4}	2.8982e-03	7.6653e-04	1.9477e-04	4.8903e-05	1.2239e-05	3.0612e-06	1.98
	2^{-6}	8.5694e-03	2.6819e-03	7.6480e-04	2.0144e-04	5.1142e-05	1.2837e-05	1.88
u_{1h}	2^{-8}	1.4824e-02	6.1724e-03	2.1760e-03	6.7869e-04	1.9303e-04	5.0798e-05	1.64
	2^{-10}	1.6786e-02	8.1129e-03	3.7374e-03	1.5503e-03	5.4621e-04	1.7008e-04	1.32
	2^{-12}	1.7276e-02	8.6066e-03	4.2326e-03	2.0364e-03	9.3615e-04	3.8820e-04	1.10
	2^{-14}	1.7398e-02	8.7299e-03	4.3564e-03	2.1604e-03	1.0602e-03	5.0956e-04	1.02
	2^{-16}	1.7429e-02	8.7606e-03	4.3872e-03	2.1913e-03	1.0911e-03	5.4044e-04	1.00
	2^{-18}	1.7436e-02	8.7679e-03	4.3945e-03	2.1985e-03	1.0984e-03	5.4774e-04	1.00
	1	2.1825e-05	5.4603e-06	1.3649e-06	3.4130e-07	8.5414e-08	2.1523e-08	2.00
	2^{-2}	2.8457e-04	7.0858e-05	1.7698e-05	4.4252e-06	1.1080e-06	2.7878e-07	2.00
	2^{-4}	2.0943e-03	5.1317e-04	1.2730e-04	3.1759e-05	7.9358e-06	1.9840e-06	2.01
	2^{-6}	9.6757e-03	2.5179e-03	6.1323e-04	1.5059e-04	3.7415e-05	9.3384e-06	2.00
u_{2h}	2^{-8}	2.0186e-02	8.0487e-03	2.5257e-03	6.5722e-04	1.6054e-04	3.9458e-05	1.80
	2^{-10}	2.3480e-02	1.1324e-02	5.1368e-03	2.0307e-03	6.3865e-04	1.6643e-04	1.43
	2^{-12}	2.4304e-02	1.2156e-02	5.9736e-03	2.8554e-03	1.2898e-03	5.0992e-04	1.11
	2^{-14}	2.4509e-02	1.2364e-02	6.1827e-03	3.0651e-03	1.4997e-03	7.1534e-04	1.02
	2^{-16}	2.4561e-02	1.2416e-02	6.2349e-03	3.1175e-03	1.5521e-03	7.6776e-04	1.00
	2^{-18}	2.4573e-02	1.2429e-02	6.2475e-03	3.1301e-03	1.5647e-03	7.8039e-04	1.00
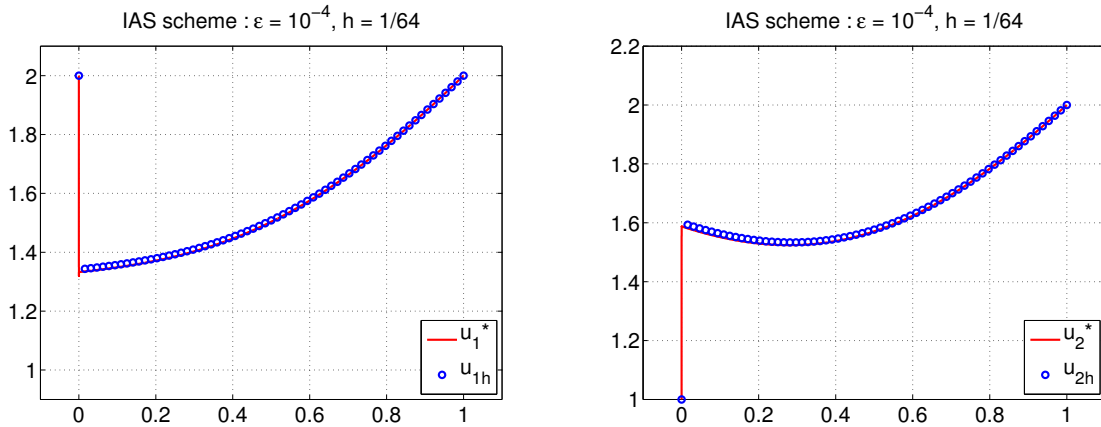
Figure 4.3. The reference solution and IAS solution of Example 4.3 with $\varepsilon = 10^{-4}$.
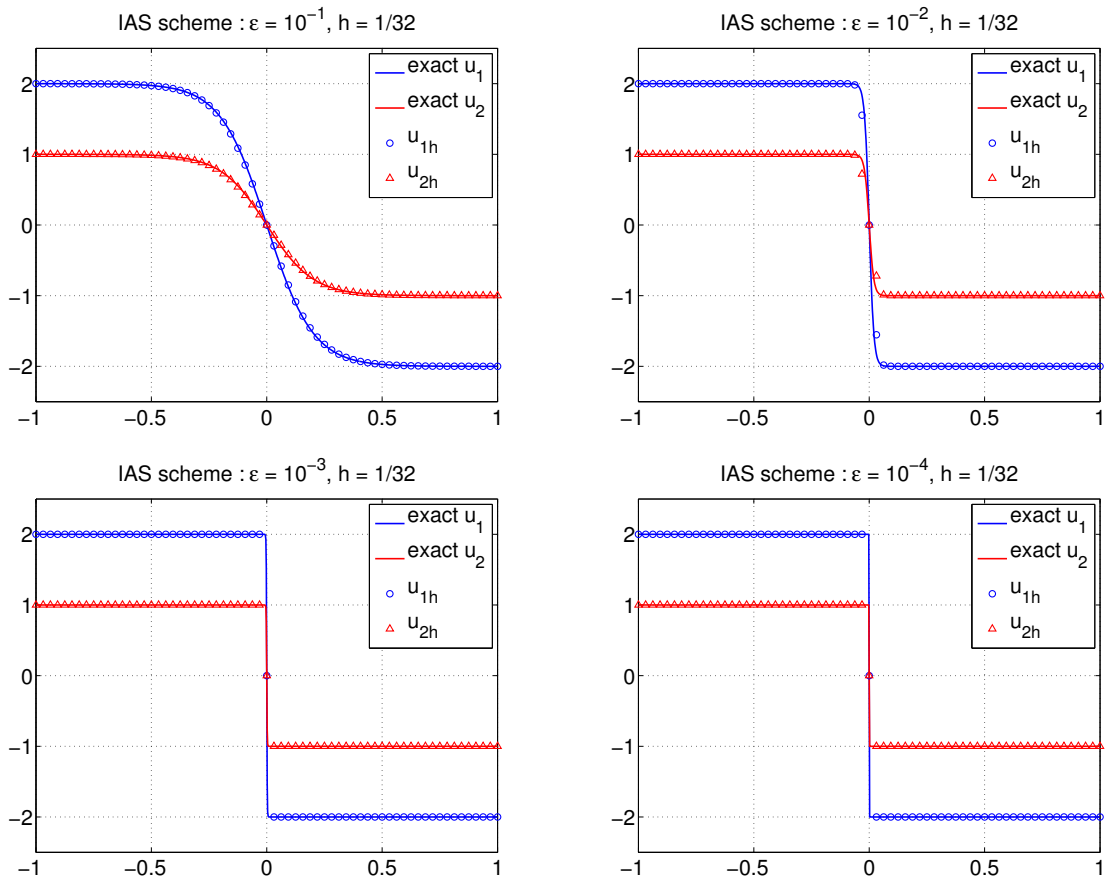
Figure 4.4. Elevation plots of the exact and IAS solutions of Example 4.4 with $\varepsilon = 10^{-\ell}$, $\ell = 1, 2, 3, 4$, on a uniform mesh with $h = 1/32$.

(see, e.g., [5, 6]):

$$-\varepsilon\Delta \begin{bmatrix} u_1 \\ u_2 \end{bmatrix} - \begin{bmatrix} 0 & a_1 \\ a_1 & 0 \end{bmatrix} \begin{bmatrix} u_1 \\ u_2 \end{bmatrix}_x - \begin{bmatrix} 0 & a_2 \\ a_2 & 0 \end{bmatrix} \begin{bmatrix} u_1 \\ u_2 \end{bmatrix}_y = \begin{bmatrix} f_1 \\ f_2 \end{bmatrix} \quad \text{in } \Omega, \tag{4.9}$$

which will be supplemented with the Dirichlet boundary conditions, where u_1 is the velocity, u_2 is the induced magnetic field; $0 < \varepsilon := 1/Ha$ and Ha is the Hartmann number; $\boldsymbol{a} = (a_1, a_2)^\top = (\sin\alpha, \cos\alpha)^\top$ and $0 \le \alpha \le \pi/2$ is the angle from the positive y-axis to the externally applied magnetic field b_0, measured in the clockwise direction. In this example we consider $\alpha = \pi/3$, which implies $\boldsymbol{a} = (\sqrt{3}/2, 1/2)^\top$, and the source functions f_1 and f_2 are determined such that the exact solution $\boldsymbol{u} = (u_1, u_2)^\top$ is given by

$$u_1(x,y) = P_1(x,y) + P_2(x,y) \quad \text{and} \quad u_2(x,y) = P_1(x,y) - P_2(x,y), \tag{4.10}$$

where P_1 and P_2 are defined by

$$\begin{aligned}
P_1(x,y) &= \left\{ \frac{-x^2}{\sqrt{3}} + \frac{4\varepsilon x}{3} - \left(\frac{-1}{\sqrt{3}} + \frac{4\varepsilon}{3} \right) \left(\frac{1 - e^{-\sqrt{3}x/(2\varepsilon)}}{1 - e^{-\sqrt{3}/(2\varepsilon)}} \right) \right\} \\
&\quad \times \left\{ -y^2 + 4\varepsilon y + (-1 + 4\varepsilon) \left(\frac{1 - e^{-y/(2\varepsilon)}}{1 - e^{-1/(2\varepsilon)}} \right) \right\}, \\
P_2(x,y) &= \left\{ \frac{x^2}{\sqrt{3}} + \frac{4\varepsilon x}{3} + \left(\frac{1}{\sqrt{3}} + \frac{4\varepsilon}{3} \right) \left(\frac{e^{-\sqrt{3}/(2\varepsilon)} - e^{\sqrt{3}(x-1)/(2\varepsilon)}}{1 - e^{-\sqrt{3}/(2\varepsilon)}} \right) \right\} \\
&\quad \times \left\{ y^2 + 4\varepsilon y + (1 + 4\varepsilon) \left(\frac{e^{-1/(2\varepsilon)} - e^{(y-1)/(2\varepsilon)}}{1 - e^{-1/(2\varepsilon)}} \right) \right\}.
\end{aligned}$$

In recent years, the study of steady incompressible MHD flow through pipes under a transverse magnetic field has found practical applications in many fields like flowmetry, MHD power generation and blood flow measurements [5, 6]. In this example, when the perturbation parameter ε is small enough, then strong boundary layer will appear on the whole boundary $\partial\Omega$. The newly developed IAS scheme performs very well, see Figure 4.5 and Table 4.4 for the numerical results of various singular perturbation parameters.

Example 4.6 (*2-D Jordan-canonical-form problem*). We construct a 2-D strongly coupled system of singularly perturbed convection-diffusion equations in the unit square $\Omega := (0,1) \times (0,1)$,

$$-\varepsilon\Delta \begin{bmatrix} u_1 \\ u_2 \end{bmatrix} - \begin{bmatrix} 1/2 & 1 \\ 0 & 1/2 \end{bmatrix} \begin{bmatrix} u_1 \\ u_2 \end{bmatrix}_x - \begin{bmatrix} \sqrt{3}/2 & 1 \\ 0 & \sqrt{3}/2 \end{bmatrix} \begin{bmatrix} u_1 \\ u_2 \end{bmatrix}_y = \begin{bmatrix} f_1 \\ f_2 \end{bmatrix} \quad \text{in } \Omega \tag{4.11}$$

subject to the Dirichlet boundary conditions. Notice that in this example, the convection coefficient matrices $\boldsymbol{A}$ and $\boldsymbol{B}$ are given by

$$\boldsymbol{A} = \begin{bmatrix} 1/2 & 1 \\ 0 & 1/2 \end{bmatrix} \quad \text{and} \quad \boldsymbol{B} = \begin{bmatrix} \sqrt{3}/2 & 1 \\ 0 & \sqrt{3}/2 \end{bmatrix}, \tag{4.12}$$

which are already posed in the Jordan canonical forms. The source functions f_1 and f_2 are

Table 4.4. Maximum errors of the IAS solutions of Example 4.5.

|	ε	$h = 2^{-5}$	$h = 2^{-6}$	$h = 2^{-7}$	$h = 2^{-8}$	$h = 2^{-9}$	$h = 2^{-10}$	order
u_{1h}	1	7.0014e-08	1.7505e-08	4.3780e-09	1.0945e-09	2.7360e-10	6.8291e-11	2.00
	2^{-2}	1.3606e-05	3.4098e-06	8.5266e-07	2.1317e-07	5.3294e-08	1.3325e-08	2.00
	2^{-4}	5.7300e-04	1.4361e-04	3.5936e-05	8.9852e-06	2.2464e-06	5.6162e-07	2.00
	2^{-6}	4.2792e-03	1.1103e-03	2.8005e-04	7.0181e-05	1.7555e-05	4.3894e-06	1.99
	2^{-8}	1.3897e-02	4.6247e-03	1.2906e-03	3.3298e-04	8.3943e-05	2.1029e-05	1.87
	2^{-10}	1.9784e-02	9.1839e-03	3.7099e-03	1.2223e-03	3.3996e-04	8.7649e-05	1.56
	2^{-12}	2.1269e-02	1.0686e-02	5.1657e-03	2.3486e-03	9.4207e-04	3.1021e-04	1.22
	2^{-14}	2.1641e-02	1.1062e-02	5.5435e-03	2.7275e-03	1.3052e-03	5.9044e-04	1.04
	2^{-16}	2.1735e-02	1.1156e-02	5.6380e-03	2.8222e-03	1.4000e-03	6.8537e-04	1.00
	2^{-18}	2.1758e-02	1.1179e-02	5.6616e-03	2.8459e-03	1.4237e-03	7.0909e-04	0.99
	2^{-20}	2.1764e-02	1.1185e-02	5.6676e-03	2.8518e-03	1.4297e-03	7.1502e-04	0.99
	2^{-22}	2.1765e-02	1.1187e-02	5.6690e-03	2.8533e-03	1.4311e-03	7.1651e-04	0.98
	2^{-24}	2.1765e-02	1.1187e-02	5.6694e-03	2.8536e-03	1.4315e-03	7.1688e-04	0.98
u_{2h}	1	8.5333e-07	2.1353e-07	5.3387e-08	1.3347e-08	3.3369e-09	8.3421e-10	2.00
	2^{-2}	4.2399e-05	1.0607e-05	2.6519e-06	6.6300e-07	1.6575e-07	4.1439e-08	2.00
	2^{-4}	6.3698e-04	1.5961e-04	3.9926e-05	9.9836e-06	2.4960e-06	6.2401e-07	2.00
	2^{-6}	4.2911e-03	1.1141e-03	2.8091e-04	7.0396e-05	1.7609e-05	4.4029e-06	1.99
	2^{-8}	1.3900e-02	4.6253e-03	1.2907e-03	3.3301e-04	8.3951e-05	2.1031e-05	1.87
	2^{-10}	1.9785e-02	9.1840e-03	3.7099e-03	1.2223e-03	3.3996e-04	8.7650e-05	1.56
	2^{-12}	2.1270e-02	1.0686e-02	5.1657e-03	2.3486e-03	9.4207e-04	3.1021e-04	1.22
	2^{-14}	2.1643e-02	1.1062e-02	5.5435e-03	2.7275e-03	1.3052e-03	5.9044e-04	1.04
	2^{-16}	2.1736e-02	1.1156e-02	5.6380e-03	2.8222e-03	1.4000e-03	6.8537e-04	1.00
	2^{-18}	2.1759e-02	1.1179e-02	5.6617e-03	2.8459e-03	1.4237e-03	7.0909e-04	0.99
	2^{-20}	2.1765e-02	1.1185e-02	5.6676e-03	2.8518e-03	1.4297e-03	7.1502e-04	0.99
	2^{-22}	2.1766e-02	1.1187e-02	5.6690e-03	2.8533e-03	1.4311e-03	7.1651e-04	0.98
	2^{-24}	2.1767e-02	1.1187e-02	5.6694e-03	2.8536e-03	1.4315e-03	7.1688e-04	0.98
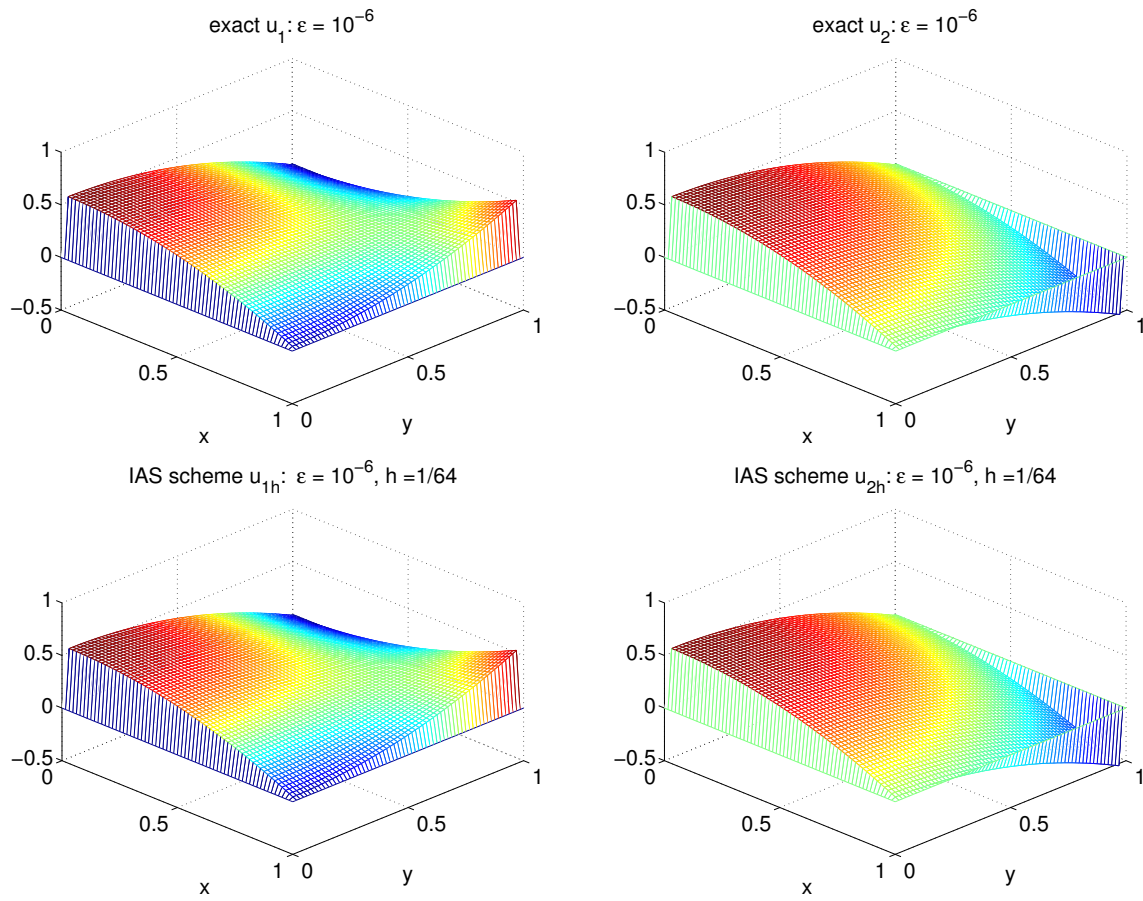
Figure 4.5. Elevation plots of the exact and IAS solutions of Example 4.5 with $\varepsilon = 10^{-6}$.

determined such that the exact solution $\boldsymbol{u} = (u_1, u_2)^\top$ is given by

$$
\begin{cases}
\begin{aligned}
u_1(x,y) &= \frac{x^2 e^{-1/(2\varepsilon)} - (x^2-1) - e^{-x/(2\varepsilon)} + 4\varepsilon(x-1-xe^{-1/(2\varepsilon)} + e^{-x/(2\varepsilon)})}{1 - e^{-1/(2\varepsilon)}} \\
&\quad \times \left\{ \frac{\sqrt{3}(y^2 e^{-\sqrt{3}/(2\varepsilon)} - (y^2-1) - e^{-\sqrt{3}x/(2\varepsilon)}) + 4\varepsilon(y-1-ye^{-\sqrt{3}/(2\varepsilon)} + e^{-\sqrt{3}x/(2\varepsilon)})}{3(1 - e^{-\sqrt{3}//(2\varepsilon)})} \right\}, \\
u_2(x,y) &= -\left\{ \frac{2(-x^3 e^{-1/(2\varepsilon)} + x^3 - 1 + e^{-x/(2\varepsilon)}) - 12\varepsilon(-x^2 e^{-1/(2\varepsilon)} + x^2 - 1 + e^{-x/(2\varepsilon)})}{3(1 - e^{-1/(2\varepsilon)})} \right. \\
&\quad \left. + \frac{48\varepsilon^2(x-1-xe^{-1/(2\varepsilon)} + e^{-x/(2\varepsilon)})}{3(1 - e^{-1/(2\varepsilon)})} \right\} \\
&\quad \times \left\{ \frac{2(-y^3 e^{-\sqrt{3}/(2\varepsilon)} + y^3 - 1 + e^{-\sqrt{3}y/(2\varepsilon)}) - 4\sqrt{3}\varepsilon(-y^2 e^{-\sqrt{3}/(2\varepsilon)} + y^2 - 1 + e^{-\sqrt{3}y/(2\varepsilon)})}{3\sqrt{3}(1 - e^{-\sqrt{3}/(2\varepsilon)})} \right. \\
&\quad \left. + \frac{16\varepsilon^2(y-1-ye^{-\sqrt{3}/(2\varepsilon)} + e^{-\sqrt{3}y/(2\varepsilon)})}{3\sqrt{3}(1 - e^{-\sqrt{3}/(2\varepsilon)})} \right\}.
\end{aligned}
\end{cases}
\tag{4.13}
$$

We can verify that when the perturbation parameter ε is small enough, both the solution components u_1 and u_2 exhibit strong boundary layers near the x-axis and y-axis.

The numerical results for various perturbation parameters are reported in Table 4.5, which confirm our prediction. Moreover, we depict the elevation plots of the exact and IAS solutions for $\varepsilon = 10^{-6}$ in Figure 4.6. Not surprisingly, the IAS scheme captures the strong boundary layers very effectively.

5 Summary and conclusions

In this paper, we have developed an IAS scheme, which appears to be a parameter-uniform difference scheme with a formally second-order accuracy, for solving strongly coupled systems of singularly perturbed convection-diffusion equations whose solutions may display strong boundary and/or interior layer behavior. By decomposing the coefficient matrix of convection term into the Jordan canonical form, we have first constructed an IAS scheme for 1-D systems and then have extended the scheme to 2-D systems on a five-point compact stencil by employing an alternating direction technique. In order to illustrate the robustness of the developed IAS scheme, we have presented a series of numerical experiments exhibiting strong boundary or interior layers. From the numerical results, we have observed that when the perturbation parameter ε is small enough, the developed IAS scheme is first order convergent in the discrete maximum norm on uniform meshes, which appears to be uniformly in ε. A further theoretical analysis is needed to validate this interesting observation.

Finally, we remark that the techniques developed in this paper can be applied to strongly coupled systems of convection-diffusion equations in higher dimensions and the case of each singularly perturbed equation in the coupled system having a different perturbation parameter.

Table 4.5. Maximum errors of the IAS solutions of Example 4.6.

	ε	$h = 2^{-5}$	$h = 2^{-6}$	$h = 2^{-7}$	$h = 2^{-8}$	$h = 2^{-9}$	$h = 2^{-10}$	order
u_{1h}	1	3.6628e-07	9.1623e-08	2.2911e-08	5.7281e-09	1.4321e-09	3.5811e-10	2.00
	2^{-2}	1.8520e-05	4.6394e-06	1.1603e-06	2.9011e-07	7.2529e-08	1.8131e-08	2.00
	2^{-4}	3.1268e-04	7.9101e-05	1.9834e-05	4.9647e-06	1.2414e-06	3.1036e-07	2.00
	2^{-6}	1.7519e-03	4.9095e-04	1.2644e-04	3.1849e-05	7.9816e-06	1.9967e-06	1.96
	2^{-8}	8.5102e-03	1.7558e-03	4.9459e-04	1.3638e-04	3.4977e-05	8.8009e-06	1.98
	2^{-10}	1.7267e-02	7.2185e-03	2.2794e-03	4.8754e-04	1.2694e-04	3.4872e-05	1.79
	2^{-12}	1.9655e-02	9.6277e-03	4.4629e-03	1.8413e-03	5.8513e-04	1.2620e-04	1.46
	2^{-14}	2.0255e-02	1.0228e-02	5.0641e-03	2.4444e-03	1.1250e-03	4.6346e-04	1.09
	2^{-16}	2.0405e-02	1.0379e-02	5.2145e-03	2.5949e-03	1.2755e-03	6.1347e-04	1.01
	2^{-18}	2.0443e-02	1.0416e-02	5.2522e-03	2.6325e-03	1.3132e-03	6.5112e-04	0.99
	2^{-20}	2.0452e-02	1.0426e-02	5.2616e-03	2.6419e-03	1.3226e-03	6.6053e-04	0.99
	2^{-22}	2.0454e-02	1.0428e-02	5.2639e-03	2.6443e-03	1.3249e-03	6.6288e-04	0.99
	2^{-24}	2.0455e-02	1.0429e-02	5.2645e-03	2.6449e-03	1.3255e-03	6.6347e-04	0.99
u_{2h}	1	1.0513e-06	2.6305e-07	6.5775e-08	1.6444e-08	4.1111e-09	1.0277e-09	2.00
	2^{-2}	2.7859e-05	6.9676e-06	1.7424e-06	4.3562e-07	1.0890e-07	2.7227e-08	2.00
	2^{-4}	4.7843e-04	1.2005e-04	3.0042e-05	7.5120e-06	1.8781e-06	4.6953e-07	2.00
	2^{-6}	2.9718e-03	7.7171e-04	1.9481e-04	4.8829e-05	1.2215e-05	3.0541e-06	1.99
	2^{-8}	8.8375e-03	2.9754e-03	8.3563e-04	2.1608e-04	5.4499e-05	1.3655e-05	1.87
	2^{-10}	1.2251e-02	5.6235e-03	2.2868e-03	7.6459e-04	2.1409e-04	5.5319e-05	1.56
	2^{-12}	1.3177e-02	6.5222e-03	3.1332e-03	1.4243e-03	5.7665e-04	1.9232e-04	1.22
	2^{-14}	1.3410e-02	6.7506e-03	3.3587e-03	1.6472e-03	7.8764e-04	3.5724e-04	1.05
	2^{-16}	1.3468e-02	6.8078e-03	3.4154e-03	1.7035e-03	8.4368e-04	4.1282e-04	1.01
	2^{-18}	1.3483e-02	6.8221e-03	3.4296e-03	1.7176e-03	8.5774e-04	4.2685e-04	1.00
	2^{-20}	1.3486e-02	6.8257e-03	3.4331e-03	1.7211e-03	8.6126e-04	4.3037e-04	0.99
	2^{-22}	1.3487e-02	6.8266e-03	3.4340e-03	1.7220e-03	8.6214e-04	4.3125e-04	0.99
	2^{-24}	1.3488e-02	6.8268e-03	3.4342e-03	1.7222e-03	8.6236e-04	4.3147e-04	0.99
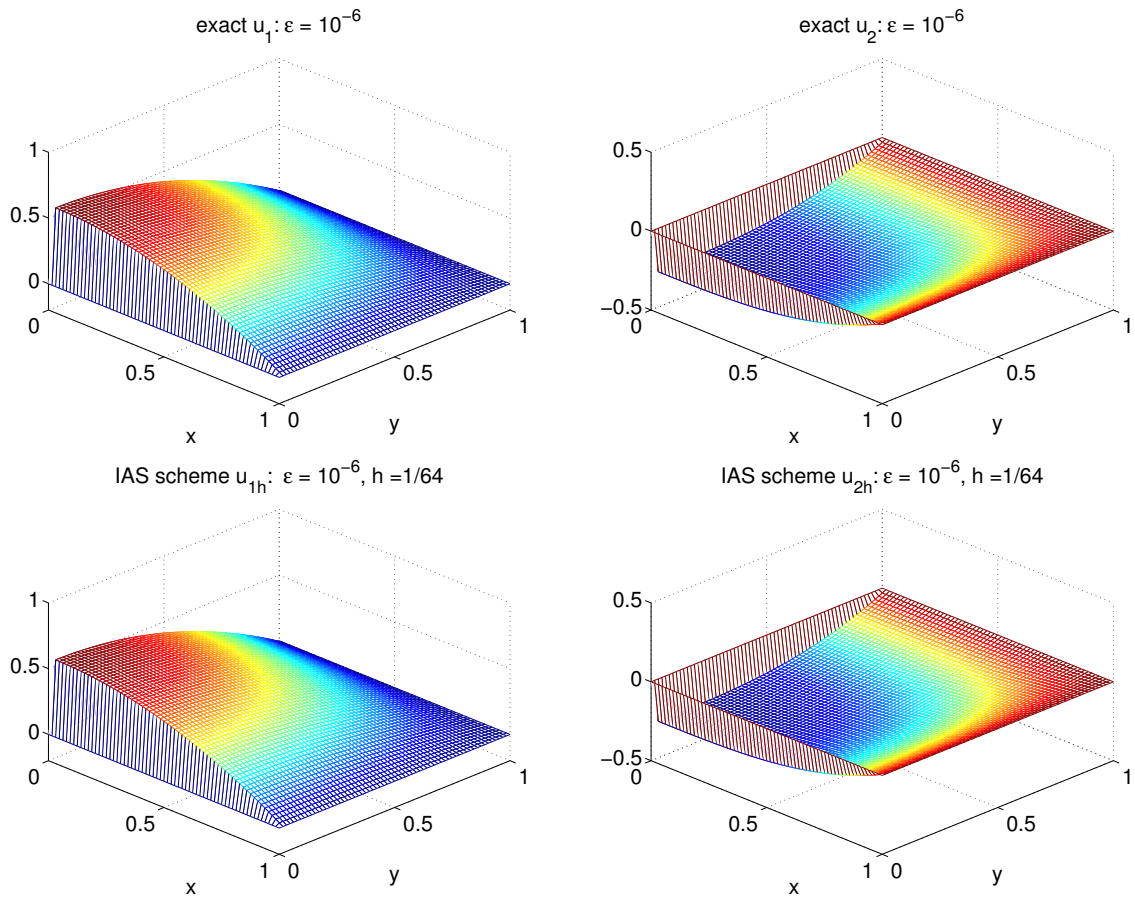
Figure 4.6. Elevation plots of the exact and IAS solutions of Example 4.6 with $\varepsilon = 10^{-6}$.

References

[1] S. Franz and H.-G. Roos, The capriciousness of numerical methods for singular perturbations, *SIAM Rev.*, 53 (2011), pp. 157-173.

[2] A. F. Hegarty, E. O'Riordan, and M. Stynes, A comparison of uniformly convergent difference schemes for two-dimensional convection-diffusion problems, *J. Comput. Phys.*, 105 (1993), pp. 24-32.

[3] P.-W. Hsieh, Y. Shih, and S.-Y. Yang, A tailored finite point method for solving steady MHD duct flow problems with boundary layers, *Commun. Comput. Phys.*, 10 (2011), pp. 161-182.

[4] P.-W. Hsieh, Y. Shih, S.-Y. Yang, and C.-S. You A novel technique for constructing difference schemes for systems of singularly perturbed equations, *Commun. Comput. Phys.*, 19 (2016), pp. 1287-1301.

[5] P.-W. Hsieh and S.-Y. Yang, Two new upwind difference schemes for a coupled system of convection-diffusion equations arising from the steady MHD duct flow problems, *J. Comput. Phys.*, 229 (2010), pp. 9216-9234.

[6] P.-W. Hsieh and S.-Y. Yang, A bubble-stabilized least-squares finite element method for steady MHD duct flow problems at high Hartmann numbers, *J. Comput. Phys.*, 228 (2009), pp. 8301-8320.

[7] R. A. Horn and C. R. Johnson, *Matrix Analysis,* Cambridge University Press, Cambridge, 1985.

[8] R. B. Kellogg, T. Linβ, and M. Stynes, A finite difference method on layer-adapted meshes for an elliptic reaction-diffusion system in two dimensions, *Math. Comput.*, 77 (2008), pp. 2085-2096.

[9] R. B. Kellogg, N. Madden, and M. Stynes, A parameter-robust numerical method for a system of reaction-diffusion equations in two dimensions, *Numer. Methods Partial Differential Eq.*, 24 (2008), pp. 312-334.

[10] R. B. Kellogg and A. Tsan, Analysis of some difference approximation for a singularly perturbed problem without turning points, *Math. Comput.*, 32 (1978), pp. 1025-1039.

[11] P. V. Kokotović, Applications of singular perturbation techniques to control problems, *SIAM Rev.*, 26 (1984), pp. 501-550.

[12] T. Linβ, Analysis of an upwind finite-difference scheme for a system of coupled singularly perturbed convection-diffusion equations, *Computing,* 79 (2007), pp. 23-32.

[13] T. Linβ, Analysis of a system of singularly perturbed convection-diffusion equations with strong coupling, *SIAM J. Numer. Anal.,* 47 (2009), pp. 1847-1862.

[14] T. Linβ and N. Madden, An improved error estimate for a numerical method for a system of coupled singularly perturbed reaction-diffusion equations, *Comp. Meth. Appl. Math.,* 3 (2003), pp. 417-423.

[15] T. Linβ and N. Madden, Accurate solution of a system of coupled singularly perturbed reaction-diffusion equations, *Computing*, 73 (2004), pp. 121-133.

[16] T. Linβ and M. Stynes, Numerical solution of systems of singularly perturbed differential equations, *Comput. Meth. Appl. Math.,* 9 (2009), pp. 165-191.

[17] N. Madden and M. Stynes, A uniformly convergent numerical method for a coupled system of two singularly perturbed linear reaction-diffusion problems, *IMA J. Numer. Anal.,* 23 (2003), pp. 627-644.

[18] S. Matthews, E. O'Riordan, and G. Shishkin, A numerical method for a system of singularly perturbed reaction-diffusion equations, *J. Comput. Appl. Math.,* 145 (2002), pp. 151-166.

[19] K. W. Morton, *Numerical Solution of Convection-Diffusion Problems*, Chapman & Hall, London, UK, 1996.

[20] E. O'Riordan and M. Stynes, Numerical analysis of a strongly coupled system of two singularly perturbed convection-diffusion problems, *Adv. Comput. Math.,* 30 (2009), pp. 101-121.

[21] E. O'Riordan, J. Stynes, and M. Stynes, A parameter-uniform finite difference method for a coupled system of convection-diffusion two-point boundary value problems, *Numer. Math. Theor. Meth. Appl.,* 1 (2008), pp. 176-197.

[22] E. O'Riordan, J. Stynes, and M. Stynes, An iterative numerical algorithm for a strongly coupled system of singularly perturbed convection-diffusion problems, in *NAA 2008, LNCS 5434*, Springer-Verlag, Berlin Heidelberg, 2009, pp. 104-115.

[23] H.-G. Roos, Ten ways to generate the Il'in and related schemes, *J. Comput. Appl. Math.,* 53 (1994), pp. 43-59.

[24] H.-G. Roos, Some remarks on strongly coupled systems of convection-diffusion equations in 2D, *arXiv:1502.04473v1 [math.NA]*, 2015.

[25] H.-G. Roos and M. Schopf, An optimal a priori error estimate in the maximum norm for the Il'in scheme in 2D, *BIT Numer. Math.,* 55 (2015), pp. 1169-1186.

[26] H.-G. Roos and M. Stynes, Some open questions in the numerical analysis of singularly perturbed differential equations, *Comput. Meth. Appl. Math.,* 15 (2015), pp. 531-550.

[27] H.-G. Roos, M. Stynes, and L. Tobiska, *Robust Numerical Methods for Singularly Perturbed Differential Equations, Second Edition*, Springer-Verlag, Berlin, 2008.

[28] G. I. Shishkin, Mesh approximation of singularly perturbed boundary-value problems for systems of elliptic and parabolic equations, *Comput. Maths. Math. Phys.*, 35 (1995), pp. 429-446.

[29] L. Shishkina and G. Shishkin, Robust numerical method for a system of singularly perturbed parabolic reaction-diffusion equations on a rectangle, *Math. Model. Anal.*, 13 (2008), pp. 251-261.

[30] M. Stephens and N. Madden, A parameter-uniform Schwarz method for a coupled system of reaction-diffusion equations, *J. Comput. Appl. Math.*, 230 (2009), pp. 360-370.

[31] M. Stynes, Steady-state convection-diffusion problems, *Acta Numerica*, 2005, pp. 445-508.

[32] G. P. Thomas, Towards an improved turbulence model for wave-current interactions, in *Second Annual Report to EU MAST-III Project "The Kinematics and Dynamics of Wave-Current Interactions,"* 1998.

[33] R. S. Varga, On a discrete maximum principle, *J. SIAM Numer. Anal.,* 3 (1966), pp. 355-359.